

(12) INTERNATIONAL APPLICATION PUBLISHED UNDER THE PATENT COOPERATION TREATY (PCT)

(19) World Intellectual Property Organization  
International Bureau



(43) International Publication Date  
22 February 2001 (22.02.2001)

PCT

(10) International Publication Number  
WO 01/13142 A1

(51) International Patent Classification<sup>7</sup>: G01V 3/00

George, Richard; 440 FM 2754, Bellville, TX 78746 (US). AADIREDDY, Prabhakar; 15131 Memorial Drive #2107, Houston, TX 77079 (US).

(21) International Application Number: PCT/US00/22252

(22) International Filing Date: 11 August 2000 (11.08.2000)

(74) Agents: MORRIS, Francis, E. et al.; Pennie & Edmonds LLP, 1155 Avenue of the Americas, New York, NY 10036 (US).

(25) Filing Language:

English

(26) Publication Language:

English

(81) Designated States (national): CA, NO.

(30) Priority Data:

60/148,943

13 August 1999 (13.08.1999) US

(84) Designated States (regional): European patent (AT, BE, CH, CY, DE, DK, ES, FI, FR, GB, GR, IE, IT, LU, MC, NL, PT, SE).

(71) Applicant: HALLIBURTON ENERGY SERVICES, INC. [US/US]; 4100 Clinton Drive, Building 01, Houston, TX 77020-6299 (US).

Published:

— With international search report.

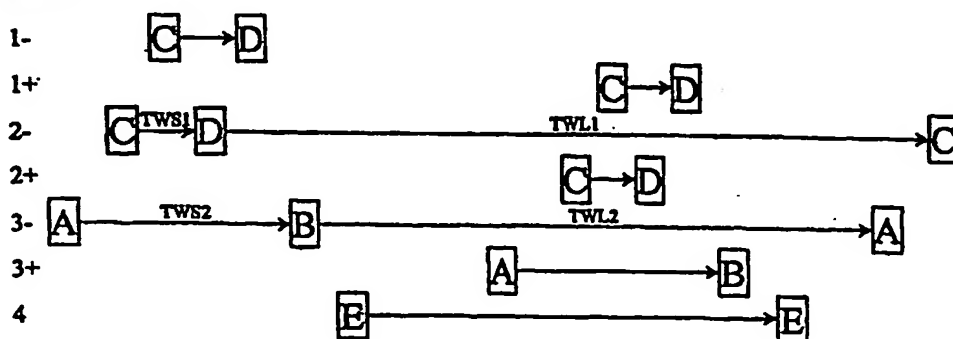
— Before the expiration of the time limit for amending the claims and to be republished in the event of receipt of amendments.

(72) Inventors: HOU, Lei, Bob; 1602 Enclave Parkway #1510, Houston, TX 77077 (US). MILLER, Daniel, Lee; 3203 Timberlark Drive, Kingwood, TX 77339 (US). GOLFORD, James, Elmer; 3311 Ashmont Lane, Missouri City, TX 77459 (US). BOUTON, John, C., Jr.; 3965 Regina Place, Doylestown, PA 18901 (US). COATES,

For two-letter codes and other abbreviations, refer to the "Guidance Notes on Codes and Abbreviations" appearing at the beginning of each regular issue of the PCT Gazette.

(54) Title: NMR APPARATUS AND METHODS FOR MEASURING VOLUMES OF HYDROCARBON GAS AND OIL

Frequency



(57) Abstract: A multifrequency method and apparatus for NMR logging. The apparatus and method uses a triple-wait-time (TWS1, TWS2, TWL1) NMR sequence to determine gas and light-oil filled porosity over a broad range of reservoir conditions. A set of conditions is derived for the selection of optimum acquisition parameters. The conditions are developed to aid in the selection of wait time combinations.

WO 01/13142 A1

**NMR APPARATUS AND METHODS FOR MEASURING  
VOLUMES OF HYDROCARBON GAS AND OIL**

**Field of the Invention**

5       The present invention relates to borehole measurements and more particularly to a system and method for detecting the presence and estimating the quantity of gaseous and liquid hydrocarbons using nuclear magnetic resonance.

**Background**

10       Various methods exist for performing measurements of petrophysical parameters in a geologic formation. Nuclear magnetic resonance (NMR) logging, which is the focus of this invention, is among the best methods that have been developed for a rapid determination of such parameters, which include formation porosity, composition of the formation fluid, the quantity of movable fluid and permeability, among others. NMR measurements are environmentally safe and are essentially unaffected by matrix mineralogy, because NMR signals from the matrix decay too quickly to be detected by the current generation NMR logging tools. Thus, unlike conventional neutron, density, sonic, and resistivity logs, NMR logs provide information only on formation fluids. Importantly, however, NMR tools are capable of directly measuring rock porosity filled with the fluids. Even more important is the unique capability of NMR tools, such as NUMAR Corporation's MRIL<sup>®</sup> tool to distinguish among different fluid types, in particular, clay-bound water, capillary-bound water, movable water, gas, light oil, medium oil, and heavy oil by applying different sets of user-adjusted measurement parameters. (MRIL is a mark of NUMAR Corporation, a Halliburton company). This ability to detect the presence and estimate the volumes of different types of fluids is becoming one of the main concerns in the examination of the petrophysical properties of a geologic formation.

25       To better appreciate how NMR logging can be used for fluid signal separation and estimating fluid volumes, it is helpful to briefly examine the type of parameters that can be measured using NMR techniques. It is well known that  
30

when an assembly of magnetic moments, such as those of hydrogen nuclei, are exposed in a NMR measurement to a static magnetic field they tend to align along the direction of the magnetic field, resulting in bulk magnetization. The rate at which equilibrium is established in such bulk magnetization upon provision of a static magnetic field is characterized by the parameter  $T_1$ , known as the spin-lattice relaxation time. Another related and frequently used NMR logging parameter is the spin-spin relaxation time  $T_2$  (also known as transverse relaxation time), which relaxation is the loss of transverse magnetization due to non-homogeneities varying in time in the local magnetic field over the sensing volume of the logging tool. Both relaxation times provide information about the formation porosity, the composition and quantity of the formation fluid, and others.

Another measurement parameter obtained in NMR logging is the diffusion of fluids in the formation. Generally, diffusion refers to the motion of atoms in a gaseous or liquid state due to their thermal energy. Self-diffusion is inversely related to the viscosity of the fluid, which is a parameter of considerable importance in borehole surveys. In a uniform magnetic field, diffusion has little effect on the decay rate of the measured NMR echoes. In a gradient magnetic field, however, diffusion causes atoms to move from their original positions to new ones, which moves also cause these atoms to acquire different phase shifts compared to atoms that did not move. This effect contributes to a faster rate of relaxation in a gradient magnetic field.

NMR measurements of these and other parameters of the geologic formation can be done using, for example, the centralized MRIL<sup>®</sup> tool made by NUMAR Corporation, a Halliburton company, and the sidewall CMR tool made by Schlumberger. The MRIL<sup>®</sup> tool is described, for example, in U.S. Pat. 4,710,713 to Taicher et al. and in various other publications including: "Spin Echo Magnetic Resonance Logging: Porosity and Free Fluid Index Determination," by Miller, Paltiel, Gillen, Granot and Bouton, SPE 20561, 65th Annual Technical Conference of the SPE, New Orleans, LA, Sept. 23-26, 1990; "Improved Log Quality With a Dual-Frequency Pulsed NMR Tool," by Chandler,

Drack, Miller and Prammer, SPE 28365, 69th Annual Technical Conference of the SPE, New Orleans, LA, Sept. 25-28, 1994. Certain details of the structure and the use of the MRIL<sup>®</sup> tool, as well as the interpretation of various measurement parameters are also discussed in U.S. patents 4,717,876; 4,717,877; 4,717,878; 5,212,447; 5,280,243; 5,309,098; 5,412,320; 5,517,115, 5,557,200; 5,696,448 and 5,936,405, all of which are commonly owned by the assignee of the present invention. The Schlumberger CMR tool is described, for example, in U.S. Pats. 5,055,787 and 5,055,788 to Kleinberg et al. and further in "Novel NMR Apparatus for Investigating an External Sample," by Kleinberg, Sezginer and Griffin, J. Magn. Reson. 97, 466-485, 1992. The content of the above patents and publications is hereby expressly incorporated by reference.

It has been observed that the mechanisms determining the measured values of  $T_1$ ,  $T_2$  and diffusion depend on the molecular dynamics of the formation fluids being tested and on the types of fluids present. Thus, in bulk volume liquids, which typically are found in large pores of the formation, molecular dynamics is a function of both molecular size and inter-molecular interactions, which are different for each fluid. Water, gas and different types of oil each have different  $T_1$ ,  $T_2$  and diffusivity values. On the other hand, molecular dynamics in a heterogeneous media, such as a porous solid that contains liquid in its pores, differs significantly from the dynamics of the bulk liquid, and generally depends on the mechanism of interaction between the liquid and the pores of the solid media. It will thus be appreciated that a correct interpretation of the measured signals can provide valuable information relating to the types of fluids involved, the structure of the formation and other well-logging parameters of interest.

If the only fluid in the formation is brine, a Carr-Purcell-Meiboom-Gill (CPMG) pulse sequence with a short inter-echo spacing ( $T_e$ ) and a long wait-time ( $T_w$ ) can be applied for porosity determination and identification of capillary-bound and free water volumes. Total porosity logging methods are available to improve the quality of data used for determining pore volumes occupied by clay-bound and/or capillary-bound water. (See, for example, Prammer, M.G., *et al.*: "Measurements of Clay-Bound Water and Total Porosity by Magnetic Resonance

Logging," paper SPE 36522 presented at the 1996 SPE Annual Technical Conference and Exhibition, Denver, Oct. 6-9). However, if hydrocarbons, such as formation oil and/or gas or filtrate from oil-based mud, coexist with brine, porosity determination and fluid typing (identification and quantification) with NMR becomes more difficult.

- 5 Additional difficulties arise from the fact that NMR measurements impose limitations on the logging speed. For example, it is known in the art that for porosity determination all stimulated fluid protons should be sampled at full polarization. Therefore, a long wait time  $T_w$  is required to completely detect the magnetization from protons in slow  $T_1$  processes. For gas and light oil under
- 10 typical formation conditions of temperature and pressure (100 - 300°F and 2,000 - 10,000 psi),  $T_1$  values of a few seconds occur at low-frequency (1- to 2-MHz) NMR. Wait times  $T_w$  of at least 10 seconds will capture nearly all the total proton magnetization arising from the individual  $T_1$  recovery rates encountered in petroleum logging. Such long wait times, combined with acceptable depth
- 15 sampling, restrict the logging speed and reduce wellsite efficiency. One approach addressing this problem is the application of prepolarization and multislice (multifrequency) acquisitions implemented in the Magnetic Resonance Imaging Logging™ MRIL-Prime tool. See Prammer, M.G., *et al.*: "Theory and Operation of a New Multi-Volume NMR Logging System," paper DD presented at the 40<sup>th</sup>
- 20 Annual SPWLA Logging Symposium, Oslo, Norway, May 30 - June 3, 1999. Still, it is believed that the capabilities of the MRIL tool have not yet been fully utilized.

Turning to the problem of fluid typing by NMR, it is known that it relies on contrasts of characteristic parameters of the fluids, such as  $T_1$ ,  $T_2$ , and

25 diffusivity. Two or more CPMG data sets, which may not be completely polarized, are usually acquired to exploit parameter contrasts among the expected fluids. Using NMR logging to determine reservoir porosity occupied by gas or light oil currently requires data simultaneously acquired from at least two CPMG sequences having different wait-times. Examples of this method are disclosed in

30

U.S. Patent 5,936,405 to the assignee of the present application. The content of this patent is incorporated herein by reference for all purposes.

Dual-wait-time and dual-frequency methods have been applied to determine gas volumes in both clean and shaley sand formations. It is known that the success of the application depends primarily on two factors. First, adequate  
5 signal-to-noise levels in an echo train difference has to be maintained so that the gas-filled porosity and its transverse relaxation time  $T_2$  can be accurately characterized. Second, methods must be available to reliably estimate the longitudinal relaxation time  $T_1$  of the hydrocarbon phase needed to apply a necessary amplitude correction to the apparent hydrocarbon-filled porosity. It is  
10 clear that data acquisition and processing methods that address these two factors with success are highly desirable.

NMR technology has been successfully applied to distinguish fluids, and significant progress has been made in determining porosity in mixed-fluid situations. The reader is directed for details to the disclosure of U.S. provisional  
15 patent application Ser. No. 60/106,259, filed October 30, 1998 to the assignee of the present application. The content of this application is incorporated herein by reference for all purposes. Still, quantitative analysis to determine actual hydrocarbon volumes present in the instrument's measurement space remains difficult because polarization corrections applied to apparent hydrocarbon  
20 volumes rely on accurate knowledge of the hydrocarbon  $T_1$ .

Several researchers have acknowledged the importance of  $T_1$  in quantitative fluid typing. Obtaining enough saturation-recovery data points to derive an accurate and precise  $T_1$  distribution of a fluid at acceptable logging speeds and vertical resolution is difficult or nearly impossible. Consequently,  
25 most quantitative analyses rely on  $T_1$  values computed from correlation functions or by the application of assumptions to measured values. One disadvantage of such methods is that formation parameters, such as temperature, pressure, and fluid viscosity, may not be accurately known. In addition, attention must be directed to the ranges for which the correlation functions are valid. Prior art  
30 methods of deriving  $T_1$  involve either dual  $T_w$ 's with one inter echo spacing  $T_e$  or

dual  $T_w$ 's with multiple  $T_e$ 's. See Akkurt, R., Prammer, M.G., and Moore, M.A.: "Selection of Optimal Acquisition Parameters for MRIL Logs," *The Log Analyst* (Nov.-Dec. 1996) 43; and Chen, S., *et al.*: "Estimation of Hydrocarbon Viscosity with Multiple TE Dual Wait-Time MRIL Logs," paper SPE 49009 presented at the 1998 SPE Annual Technical Conference and Exhibition, New Orleans, Sept. 27-30. Both methods referenced above assume that oil (or unpolarized brine)  $T_2$  signals are totally separated from brine  $T_2$  signals, which assumption is sometimes incorrect. Methods for obtaining gas  $T_1$  values from NMR logs have not been previously developed.

In addition to being an important parameter for correcting apparent volumes of fluids for under-polarization,  $T_1$  computations play an important role in distinguishing one fluid from another. For example, it is well known that gas and light oil have large  $T_1$  values, and thus can be separated from brine, which typically has lower values for  $T_1$ . Furthermore, fluid viscosity and self-diffusion coefficient  $D$  that can be obtained from a known  $T_1$  value can be used to separate gas from other fluids. Thus, large values for both  $T_1$  and  $D$  reliably indicate the presence of gas or light oil in a formation. Fluid viscosity can also be used in grouping liquids. Various additional contrast mechanisms are known in the art and are described, for example, in the above-referenced U.S. provisional application 60/106,259, filed October 30, 1998 to the assignee of the present application. Because  $T_1$  relaxation times are not influenced by interactions between magnetic gradients and molecular diffusion, fluid viscosities obtained from measured  $T_1$ 's are believed to be superior to other methods whenever a gradient-field logging tool is used or an internal magnetic gradient from the formation is present.

In view of the shortcomings of the prior art briefly outlined above, it is apparent that there is a need for a method and system that can take full advantage of the flexibility provided by current-generation NMR tools to enable the accurate calculation of  $T_1$  and  $T_2$  parameters for different fluids over the range of geologically meaningful values. This calculation in turn will enable reliable

30

detection of the presence of gaseous and liquid hydrocarbons and estimation of their quantities.

### Summary of the Invention

Accordingly, it is an object of the present invention to provide a method  
5 and apparatus using nuclear magnetic resonance (NMR) techniques that obviate problems associated with the prior art.

In particular, a new triple-wait-time, multi-frequency acquisition method is disclosed and successfully tested. The method takes advantage of the multi-frequency operation of modern NMR logging tools to improve the signal-to-noise  
10 ratio of the received signals at high logging speeds. Further, the acquisition method enables accurate estimation of volumes for hydrocarbon and/or free water in addition to traditional clay-bound and capillary-bound water volumes.

The new acquisition method uses optimized wait times to obtain better signal-to-noise ratios in echo train differential signals at faster logging speeds and  
15 acceptable vertical resolution. In turn, these signals can be used to determine formation fluid volumes, as well as estimates of hydrocarbon  $T_1$ . Experiments performed on a mixture of dodecane ( $C_{12}H_{26}$ ) and doped water,  $C_{12}H_{26}$  and brine in a sandstone core, and fresh water produced fluid volumes with absolute errors of less than 1.5% for echo train differences with a signal-to-noise ratio larger than  
20 4:1.

In another aspect, the present invention provides a data processing method that enables the accurate determination of both  $T_2$  and  $T_1$  parameters of hydrocarbons based on the use of at least two difference NMR signals obtained at different wait times. The data acquisition and processing method of the present  
25 invention enable the determination of gas- and light-oil-filled porosity over a broad range of reservoir conditions. In another aspect, the present invention provides a decision mechanism to help in the selection of optimum acquisition parameters for logging applications.

In particular, in accordance with the present invention is provided a  
30 (NMR) data acquisition method, comprising: providing a first set of CPMG



pulses associated with a first relatively short recovery time  $T_{WS1}$ ; providing a second set of CPMG pulses associated with a second relatively short recovery time  $T_{WS2}$ , where  $T_{WS2}$  is longer than  $T_{WS1}$ ; providing a third set of CPMG pulses associated with a relatively long recovery time  $T_{WL1}$ ; receiving NMR echo signals from a population of particles in response to the first, second and third sets of CPMG pulses; and processing the received NMR echo signals to provide a data representation associated with the longitudinal relaxation time constant  $T_1$  of the population of particles.

In specific embodiments, the steps of providing the first, second and third sets of CPMG pulses are interleaved in time and/or are acquired in different sensitive volumes. In these embodiments, the steps of providing the first, second and third sets of CPMG pulses are performed using a multi-frequency NMR logging tool. In different specific embodiments CPMG pulses associated with different recovery times may have either same or different operating frequencies. In a preferred embodiment, the first and second short recovery times  $T_{WS1}$  and  $T_{WS2}$  are selected long enough to substantially polarize a water phase component in the population of particles, or in such manner that water-phase contribution is substantially canceled in a difference signal formed by subtracting NMR signals corresponding to a relatively short recovery time from NMR signals corresponding to the relatively long recovery time  $T_{WL1}$ .

In another aspect, in accordance with the present invention is provided a method for conducting NMR logging measurements, comprising: providing a data acquisition sequence comprising at least two sets of CPMG pulses having relatively short recovery times  $T_{WS1}$  and  $T_{WS2}$ , respectively, and at least one set of CPMG pulses having relatively long recovery time  $T_{WL1}$ ; receiving NMR echo signals from a population of particles in a geologic formation in response to the provided sets of CPMG pulses; processing the received NMR echo signals to determine a first and a second apparent volumes for at least one hydrocarbon fluid phase of the geologic formation, said first apparent volume being determined from a data representation associated with signals having short recovery time  $T_{WS1}$ , and the second apparent volume being determined from a data

representation associated with signals having short recovery time  $T_{WS2}$ ; providing a data representation associated with the longitudinal relaxation time constant  $T_1$  of said at least one hydrocarbon fluid phase based on the determined first and second apparent volumes.

5 In a specific embodiment processing the received NMR echo signals comprises: forming a first difference signal  $Edif1$  by subtracting NMR signals having relatively short recovery time  $T_{WS1}$  from NMR echo signals having relatively long recovery time  $T_{WL}$ ; computing  $T_2$  distribution of the first difference signal  $Edif1$ ; and determining a value for the  $T_2$  relaxation time of said at least one hydrocarbon phase. In another embodiment, the method further comprises  
10 forming a second difference signal  $Edif2$  by subtracting NMR signals having relatively short recovery time  $T_{WS2}$  from NMR echo signals having relatively long recovery time  $T_{WL}$ . In a preferred embodiment, the method further comprises the step of computing the total porosity of the formation  $\phi_t$  from the total apparent  
15 porosity  $\phi_{ta}$  and apparent volume corrections computed based on the provided data representation associated with the longitudinal time constant(s)  $T_1$  of the fluid phases.

In another aspect, the present invention is a method of operating a multi-volume NMR logging tool, comprising: (a) acquiring a first NMR echo train or  
20 sets of echo trains in a first sensitive volume of the tool, said first echo train(s) carrying information about NMR signals with recovery time  $T_{WS1}$ ; (b) acquiring a second NMR echo train or sets of echo trains in a second sensitive volume of the tool, said second echo train(s) carrying information about NMR signals having  
25 recovery time  $T_{WL}$ ; (c) acquiring a third NMR echo train or sets of echo trains, said third echo train(s) carrying information about NMR signals with recovery time  $T_{WS2}$ ; (d) computing values for the transverse relaxation time  $T_2$  and apparent volume for at least one hydrocarbon fluid phase based on the acquired NMR echo  
30 trains; and (e) providing a data representation associated with the longitudinal relaxation time constant  $T_1$  of said at least one hydrocarbon fluid phase based on the determined first and second apparent volumes.

In another aspect, the present invention is a NMR data processing method for use in borehole logging, comprising: selecting values for a second relatively short recovery time  $T_{WS2}$  using a known functional relationship based on estimates of: (a) a first relatively short recovery time  $T_{WS1}$  needed to polarize  
5 water signals in a geologic formation surrounding the borehole; and (b) expected  $T_1$  values for hydrocarbon fluid phases in the geologic formation surrounding the borehole; providing a data acquisition sequence comprising at least two sets of CPMG pulses having said relatively short recovery times  $T_{WS1}$  and  $T_{WS2}$ , respectively, and at least one set of CPMG pulses having relatively long recovery  
10 time  $T_{WL}$ ; processing NMR echo signals received in response to the data acquisition sequence to provide an estimate of the true values for the longitudinal relaxation time constant  $T_1$  of hydrocarbon fluid phases in the geologic formation, wherein the accuracy of the estimates of the  $T_1$  constant is controlled in the step of selecting.

15

20

25

30

### Brief Description of the Drawings

The present invention will be understood and appreciated more fully from the following detailed description taken in conjunction with the drawings in which:

FIG. 1 is an illustration of the triple-wait time activation sequence used in a preferred embodiment of the present invention;

FIG. 2 is a flow diagram illustrating the data processing method used in a preferred embodiment of the present invention;

FIG. 3 is an illustration of hypothetical saturation recovery curves for water, hydrocarbon phase and a mixture of water and the hydrocarbon phase used in a specific embodiment of the present invention;

FIG. 4 are waiting time  $T_{WS2} - T_{WS1}$  cross-plots that can be used in accordance with the present invention for the selection of optimum logging acquisition parameters;

FIG. 5 is an overlay of triple-wait-time echo trains obtained from CPMG experiments performed in experiments performed on a 1.26:1 mixture of doped water and  $C_{12}H_{26}$  for different  $T_w$ ;

FIG. 6 is a  $T_2$  distribution, selected at random, from one of the 8-s  $T_w$  CPMG experiments performed on a doped-water/ $C_{12}H_{26}$  mixture;

FIG. 7 shows overlays of difference echo trains for 30 CPMG triple-wait-time sequences performed on a doped-water/ $C_{12}H_{26}$  mixture using the method of the present invention;

FIG. 8 is overlay of triple-wait-time echo trains obtained in accordance with the present invention in a laboratory setting from 28 CPMG experiments performed on a 22-p.u. sandstone core filled with a 4% KCl brine and  $C_{12}H_{26}$ ;

FIG. 9 is a  $T_2$  distribution from a 6-s  $T_w$  measurement performed on the brine- and  $C_{12}H_{26}$ -filled sandstone core in accordance with the present invention;

FIG. 10 shows overlays of difference echo trains for 28 CPMG triple-wait-time sequences performed on the brine- and  $C_{12}H_{26}$ -filled sandstone core sample, along with matched-filter curves;

FIG. 11 illustrates an improvement in signal-to-noise ratio of Edifl echo differences using the multifrequency triple-wait-time acquisition method of the present invention, compared with those obtained with a dual- $T_w$ , dual frequency method.

FIG. 12 is a block diagram of the apparatus in accordance with a preferred  
5 embodiment, which shows individual block components for controlling data collection, processing the collected data and displaying the measurement results.

10

15

20

25

30

## Description of Preferred Embodiments

### A. Equipment

In accordance with the present invention, NMR measurements are made using tools capable of performing separate, quasi-simultaneous measurements in different sensitive volumes by switching the operating frequency of the tool.

5 Fig. 12 is a block diagram of a generic system used in accordance with the present invention, and shows individual block components for controlling data collection, for processing the collected data and displaying the measurement results. As shown in Fig. 12, the system has a portion 32 (generally comprising a magnet array and antenna(s)) which is arranged to be lowered into a borehole. The tool's  
10 electronic section 30 comprises a probe controller and pulse echo detection electronics. The output signal from the detection electronics is processed by data processor 52 to analyze the relaxation characteristics of the material being investigated in the sensitive volume, generally designated as 34. The output of the data processor 52 is provided to the parameter estimator 54. Generally, data  
15 processor 52 selects the desired data acquisition technique and the corresponding set of measurement parameters.

Dependent on the selected data acquisition technique, measurement cycle controller 55 provides an appropriate control signal to the probe. In a specific embodiment, data from the log measurement is stored in data storage 56. In a  
20 preferred embodiment, raw data received by the tool can be pre-processed downhole by the electronic section 30. Data processor 52 is connected to display 58, which is capable of providing a graphical display of one or more measurement parameters, possibly superimposed on display data from data storage 56.

For the purposes of this invention it is important that the tool is capable of  
25 "hopping" from one operating frequency to another, the effect of which is to shift the radial position of the resonant volume of the tool. The frequency shift is selected in such manner that two or more non-overlapping resonant volumes are formed; each new resonant volume associated with a different frequency being filled with fully relaxed protons. Hopping between two or more (i.e., K)  
30 frequencies thus allows reducing the time between experiments approximately by

a factor of K, without compromising complete  $T_1$  measurements or adopting imprecise empirical  $T_1/T_2$  relationships; the logging speed for the tool can accordingly be increased approximately K times.

The components of the system of the present invention shown in Fig. 12 can be implemented in hardware or software, or any combination thereof suitable for practical purposes. Preferably, the data processing algorithms used in accordance with the invention are programmed into software which is stored in a computer storage medium for execution on a computer, such as data processor 52. In a preferred embodiment, NMR measurements in accordance with the present invention are done using Numar Corporation's (a Halliburton Company) MRIL® tools having multi-frequency capability, such as the MRIL® -Prime tool. Details of the structure, the operation and the use of logging tools, as illustrated in Fig. 12, are also discussed, for example, in U.S. patents 4,717,876; 4,717,877; 4,717,878; 5,212,447; 5,280,243; 5,309,098; 5,412,320; 5,517,115; 5,557,200; 5,696,448 and 5,936,405 to the assignee of the present application, the contents of which are incorporated herein for all purposes.

#### **B. Data acquisition**

In accordance with a preferred embodiment of the present invention, the multi-frequency capability of the operating tool is used to provide a new data acquisition method, which is particularly suitable for the detection of gas and other hydrocarbons on the basis of NMR measurements with different wait times  $T_w$ . To this end, with reference to Fig. 1, a novel interleaved pulse sequence is proposed using triple-wait-time activation.

Fig. 1 generally illustrates a method for measuring volumes occupied by hydrocarbons, and in particular shows a triple-wait-time activation sequence of the preferred embodiment. As shown, the activation sequence used in a preferred embodiment of the present invention uses seven resonant frequencies, which are grouped into four frequency bands designated 1, 2, 3, and 4. The specific frequencies used in these four bands depend on the characteristics of the tool and the desirable sensitive volume. In a specific embodiment using Numar

Corporation's MRIL tool, the nominal center frequencies for bands 1, 2, 3 and 4 shown in Fig. 1 are 620 kHz, 650 kHz, 680 KHz and 760 kHz, respectively. As shown, in a preferred embodiment of the method there are two frequencies each corresponding to frequency bands 1, 2, and 3. These two frequencies, denoted in Fig. 1 by plus and minus signs appended to the band number, are +6 and -6 kHz  
5 relative to the band center frequency in a specific embodiment. In the embodiment illustrated in Fig. 1, band 4 is a single frequency band that operates at a nominal frequency of 760 kHz for the MRIL tool. It can be shown that in this embodiment the radial distance between the inner- and outer-most sensitive volumes is less than one inch.

10 For ease of notation, data groups acquired using identical wait times  $T_w$  have identical labels, and are designated A, B, C, D and E. As shown in Fig.1, in general there are four wait times involved in the measurements performed at the 1-, 1+, 2-, 2+, 3-, and 3+ frequencies - two relatively short wait times designated  $T_{WS1}$  and  $T_{WS2}$ , and two relatively long wait times,  $T_{WL1}$  and  $T_{WL2}$ . However, at  
15 normal logging speeds measurement volumes with these frequencies are completely replenished with protons that have been fully polarized during the  $T_{WL1}$  and  $T_{WL2}$  delays. For example, this may be due to the length of the wait time interval and/or the use of pre-polarizing magnets. Thus, for practical purposes the activation sequence of the present invention effectively involves only one long  
20 wait time  $T_{WL}$ , which is used for data processing purposes. In a preferred embodiment this wait time  $T_{WL}$  is selected as the longest delay time  $T_{WL1}$  shown in Fig. 1.

In accordance with the present invention, and with further reference to Fig. 2, four frequencies (1-, 1+, 2-, and 2+) in the activation sequence shown in  
25 Fig. 1 provide improved signal-to-noise ratio in echo train differences compared with prior art data acquisitions made with dual-frequency tools. As explained below, measurements performed at these frequencies (data groups C and D) are generally used to obtain  $T_2$  estimates and apparent hydrocarbon volumes. On the other hand, NMR signals obtained from the combination of the 1-, 1+, 2-, 2+, 3-,  
30 and 3+ frequencies (data groups A, B, C and D) are used in accordance with the



present invention to determine hydrocarbon  $T_1$  values. In turn, these values are used to make polarization corrections to apparent hydrocarbon volumes derived from the 1-, 1+, 2-, and 2+ frequency measurements.

In a preferred embodiment, measurements at frequency band 4 (data groups E in Fig. 1) consist of a small number of high-quality echoes. Data groups E are used to improve the precision in measuring rapid  $T_2$  decay components usually associated with clay-bound water and/or capillary-bound water.

In accordance with the present invention, the design of the activation sequence illustrated in a preferred embodiment in Fig. 1 also improves the logging speed of the tool. It is known in the art that under the influence of tool motion, RF, magnetic field values, and sensitive volume can not be constant at a particular location in a formation. See, for example, Edwards, C.M.: "Effects of Tool Design and Logging Speed on  $T_2$  NMR Log Data," paper RR presented at the 38<sup>th</sup> Annual SPWLA Logging Symposium, Houston, June 15–18, 1997. As a consequence, apparent  $T_2$  values decrease with increasing logging speed. It is clear that the addition of more frequencies (measurement volumes) in accordance with the present invention causes a larger volume of formation to be sampled per unit length of tool motion, so that a greater signal-to-noise ratio (SNR) is attained. In the alternative, for a given SNR one can obtain higher logging speed. It has been determined that for the acquisition sequence illustrated in Fig. 1, using the MRIL tool of the preferred embodiment, the maximum logging speed is about 900 ft/hr, which gives a vertical resolution of approximately 3 ft and minimizes the influence of logging speed on  $T_2$  determination.

It will be appreciated by those of skill in the art that in alternative embodiments of this invention a different, for example larger, number of frequency bands and/or frequencies per band can be used in the activation sequence. It should be apparent that in such alternative embodiments one can increase the SNR of the received signals by combining more data groups per data point. For example, with reference to Fig. 1, instead of two data groups C for the first data point (one at frequency band 1- and one at frequency band 2-) one can use a higher number. In an alternative embodiment, a single data group can be

used per data point. As illustrated in Fig. 1, data for the three different recovery times need not necessarily be obtained from only three different frequencies. For example, two or more measurements associated with different frequencies can be combined (i.e., averaged) to result in a single data stream corresponding to either a short, or a long recovery time. Additional modifications in the parameters of the pulse sequences can be applied, as known in the art. For example, it is known that the contrast between liquid and gas signals can be enhanced by using a slightly larger pulse-echo spacing for the CPMG train associated with the shorter recovery interval. Modifications of this type are straightforward extensions of the activation sequence illustrated in Fig. 1.

The activation sequence illustrated in a preferred embodiment in Fig. 1 is believed to have at least two significant advantages over the prior art, including dual- $T_w$ , dual-frequency methods for determining volumes of gas or light oil. First, the addition of more frequencies (measurement volumes) causes a larger volume of formation to be sampled per unit length of tool motion so that a greater signal-to-noise ratio (SNR) is attained in the echo train differential signals used to determine apparent hydrocarbon volumes. Second, the acquisition sequence has the important advantage that interlaced measurements having three wait times enable the computation of  $T_1$  values for the hydrocarbon phases in the formation, as shown below.

### C. Data processing

In accordance with a preferred embodiment of the present invention, data acquired with the new activation sequence discussed above is processed as shown in Fig. 2. In particular, at step 10 raw echoes are received according to a triple-wait-time activation sequence, such as shown in Fig. 1. In step 20, in a preferred embodiment the method applies certain corrections to the raw data generally designed to improve the signal-to-noise ratio of the received signal. In a specific embodiment, in step 20 the raw data undergoes a phase correction and/or a running average correction. Both corrections are known in the art and thus will not be considered in detail. For purposes of illustration, in a specific embodiment implementing phase correction, if  $r(n)$  is the magnitude for the  $n$ th echo in a CPMG echo train, and  $a(n)$  is its angle (in radians) the phase correction for the CPMG echo train is given by the following pseudo-code:

- 1) First find the Phase correction angle  $A$  over a group of  $M$  echos (where  $M = 2-10$  in a specific embodiment)

$$R \cdot \exp(j \cdot A) = \sum [r(n) \cdot \exp(j \cdot a(n))], n=1, \dots, M,$$

- 2) Apply phase correction, i.e., phase rotation to the individual echos using

$$r(n) \cdot \exp(j \cdot a(n)) \cdot \exp(-j \cdot A)$$

- 3) obtain phase corrected values using  
 $\text{Echoes} = \text{Re}\{r(n) \cdot \exp(j \cdot a(n)) \cdot \exp(-j \cdot A)\}$   
 where  $\text{Re}\{.\}$  is taking the real part.

It will be appreciated that the above processing sequence separates signal with noise in one channel and noise only in the secondary channel (i.e., the imaginary part following the correction), and has the additional benefit of reducing the original complex number representation to working with real numbers.

In a specific embodiment, a running average correction (using 8 or 16 echos) can also be applied as known in the art in step 20 to further improve the signal-to-noise ratio.

With reference to Fig. 2, following step 20 the processing algorithm is separated into two branches. Generally, hydrocarbon volumes and  $T_1$  estimates are determined in the right branch. In the left branch, the long  $T_w$  and frequency 4 echo data are inverted to obtain  $T_2$  distributions that are combined to obtain an apparent total porosity, capillary- and clay-bound water volumes, and other parameters of interest.

Focusing first on the determination of hydrocarbon volumes, in accordance with the present invention the method generally comprises four steps. First, the  $T_2$ 's of the hydrocarbons are determined. In the second step, the determined  $T_2$ 's are used to extract hydrocarbon signal amplitudes from two echo difference trains. In accordance with the present invention these amplitudes are used to compute  $T_1$  values for the hydrocarbons, as shown below. Corrections for hydrogen index and polarization ( $T_1$ ) are applied to the signal amplitudes in the last step to compute the hydrocarbon volumes. In the left processing branch, apparent total pore (or fluid) volume  $\phi_a$  is derived from the  $T_{wL}$  and frequency 4  $T_2$  distributions. Corrected total pore volume  $\phi_i$  is then computed as the sum of  $\phi_a$  and hydrocarbon volume corrections ( $\Delta\phi_o$  and  $\Delta\phi_g$ ) that are functions of the  $T_1$ 's and hydrogen indices of the hydrocarbon phases. An additional correction ( $\Delta\phi_w$ ) may be required for under-polarized water, before various other parameters of interest are determined.

In particular, at step 30 of the method is formed the difference  $Edif1$  between echo signals with a long wait time  $T_{wL}$  and the first short wait time  $T_{ws1}$ . As shown in Fig. 1, in a preferred embodiment two or more measurements (data groups) associated with different frequencies can be combined (i.e., averaged) to result in a single data stream. Again with reference to Fig.1, forming the difference  $Edif1$  corresponds to forming differences between echo signals in the C and D data groups. It will be appreciated by those skilled in the art that the difference signal carries information essentially about the hydrocarbon phase

which has a single  $T_1$  and  $T_2$  values, because the water contribution is canceled out. In the following step 40 is computed the  $T_2$  spectrum of the Edif1 difference signal. Various ways of computing this spectrum are known in the art. In a preferred embodiment, one can use the MAP algorithm as disclosed in U.S. Pat. No. 5,517,115 to the assignee of the present application, or in Prammer, M.G.:

5 "NMR Pore Size Distributions and Permeability at the Well Site," paper SPE 28368 presented at the 1994 SPE Annual Technical Conference and Exhibition, New Orleans, Sept. 25–28. The contents of these publications are incorporated herein by reference.

In step 50 of the method are determined  $T_2$  values for the corresponding  
10 hydrocarbon components from the  $T_2$  spectrum of the difference signal. In a specific embodiment, this involves locating the peaks of the  $T_2$  spectrum and assigning the values for the peak(s) as the  $T_2$  values of the respective hydrogen components. It will be appreciated that relatively long  $T_2$  peak values generally correspond to oil components, while relatively short  $T_2$  values generally  
15 correspond to gas components.

Having determined the value(s) for the  $T_2$  of the hydrocarbon components, in the following steps 60-90 the difference signals Edif1 and Edif2 are used to compute two apparent hydrocarbon volumes. In a preferred embodiment, this is done by using matched filters to fit exponential terms to each echo difference  
20 train. First, in step 80 is formed the Edif2 difference signal between the  $T_{wL}$  and  $T_{wS2}$  signals. With reference to Fig.1 this corresponds to forming the difference between the A and B data groups. It will be appreciated that  $T_{wS2}$  is longer than  $T_{wS1}$ .

Next, the apparent hydrocarbon signal amplitudes (gas and/or oil),  $A_o$ , in  
25 the Edif1 and Edif2 echo difference trains are obtained by fitting the equation with matching filter, in this case  $\exp(-t/T_{2mp})$ , for gas and oil:

$$A(t) = A_o e^{-\frac{t}{T_{2mp}}}, \quad (1)$$

30

where  $A(t)$  represents the average echo difference amplitude at echo time  $t$  and  $T_{2mp}$  is the most probable amplitude  $T_2$  value, determined from step 50 for a hydrocarbon zoom, for the hydrocarbon phase component (gas or oil). On output, method steps 70 and 90 will give the two apparent hydrocarbon signal amplitudes  $A_0$ , corresponding to the two difference signals (Edif1 and Edif2).

- 5           Next, in step 100 of the method is determined the value for the  $T_1$  parameter(s) for the hydrocarbon phases, using the following equation (separately for oil (phase p1) and gas (phase p2)):

$$10 \quad \frac{e^{-\frac{T_{WS1}}{T_{1,p1,2}}} - e^{-\frac{T_{WL}}{T_{1,p1,2}}}}{e^{-\frac{T_{WS2}}{T_{1,p1,2}}} - e^{-\frac{T_{WL}}{T_{1,p1,2}}}} = \frac{A(T_{WS1}, T_{WL}, T_{1,p1,2})}{A(T_{WS2}, T_{WL}, T_{1,p1,2})} \quad (2)$$

- where  $A(T_{WS1}, T_{WL}, T_{1,p1,2})$  represents the apparent hydrocarbon amplitude from Edif1, and  $A(T_{WS2}, T_{WL}, T_{1,p1,2})$  is the apparent hydrocarbon amplitude from Edif2. In the case when there is only one hydrocarbon phase, Eqn. (2) above reduces to:

$$20 \quad \frac{e^{-\frac{T_{WS1}}{T_{1,p1}}} - e^{-\frac{T_{WL}}{T_{1,p1}}}}{e^{-\frac{T_{WS2}}{T_{1,p1}}} - e^{-\frac{T_{WL}}{T_{1,p1}}}} = \frac{A(T_{WS1}, T_{WL}, T_{1,p1})}{A(T_{WS2}, T_{WL}, T_{1,p1})} \quad (3)$$

- The  $T_1$ 's from the triple-wait-time experiments are found by solving Eqn. (2) or Eqn. (3) when  $A(T_{WS1}, T_{WL}, T_{1,p1})$  and  $A(T_{WS2}, T_{WL}, T_{1,p1})$  are replaced with the Edif1 and Edif2 signal amplitudes, respectively, for each experiment. The most probable value for  $T_{1mp}$  in a hydrocarbon zoom of formation, is then used in step 110 to compute corrected hydrocarbon volumes  $\phi_h$ . In a preferred embodiment, this is done by applying

30

$$\phi_h = \frac{A_{o, Ed/f}}{HI_h \left( e^{-\frac{T_{HY1}}{T_{imp}}} - e^{-\frac{T_{HY2}}{T_{imp}}} \right)}, \quad (4)$$

where  $HI_h$  is the hydrogen index of the hydrocarbon phase. In a specific embodiment, the most probable value  $T_{imp}$  is found as average over a number M of experiments, where for example,  $M = 30$  which corresponds to data points acquired in a hydrocarbon zone of formation. It will be appreciated that in alternative embodiments the hydrogen index correction can be obtained using different methods from the known parameters.

Turning next to the left branch of the processing algorithm illustrated in Fig. 2, in step 120 is determined the total apparent porosity  $\phi_{ta}$ , using  $T_{WL}$  and frequency 4  $T_2$  distributions. In a specific embodiment, the determination is done by combining a long  $T_w$  (i.e., data group A and/or C) and frequency 4 echo data (data group E). In a specific embodiment, the combination is done by separately computing the  $T_2$  spectra of the two echo signals and generating a composite signal where below certain limit, i.e., 4 ms, data group E is used, while above that merge point the  $T_{WL}$  distribution is applied. In alternative preferred embodiment, the combination is done entirely in the time domain, as described in U.S. Provisional Application 60/098,596, filed August 31, 1998 to the assignee of the present application. The content of this application is incorporated herein by reference.

In the following step 130 the total porosity  $\phi_t$  is computed from the total apparent porosity  $\phi_{ta}$ , and corrections for HI and polarization of water and hydrocarbons based on the apparent fluid volumes and  $T_1$ s computed in the right processing branch. In a specific embodiment, corrected total porosity is obtained using the corrections in Eqn. (4). Thus, for example, oil and gas corrections can be computed in a specific embodiment by  $\phi_h * \exp(-T_{WL} / T_{imp})$ . In certain instances correction for under-polarized water can be computed as a fluid phase in the right branch of the algorithm. Alternative corrections for water can be applied as known in the art.

In the following step 140 is determined the total water volume as the difference between the total porosity and the total hydrocarbon volume. From the quantities determined thus far, in the final step 150 of the algorithm are computed various parameters of interest, as shown in a specific embodiment in Fig. 2.

The data processing method illustrated in Fig. 2 is a preferred embodiment designed to operate with the data acquisition sequence in Fig. 1. Alternative embodiments are possible and will be apparent to persons of skill in the art. For example, the individual steps discussed above can be implemented using alternative signal models and/or approaches. Thus, the specific use of equations (1) - (4) is not required in accordance with the present invention. For example, once the water contribution is canceled out, in the right branch of the algorithm one may consider different signal models, with increased number of parameters for increased accuracy.

#### 15 D. Examples

The application of the new method for determining the hydrocarbon  $T_1$  values is next illustrated in the following two cases.

Case 1: A two-phase mixture, consisting of water and light oil (possibly oil filtrate) or water and gas.

20 Following echo train correction, two echo train differences, Edif1 and Edif2, are used to eliminate the broadly distributed water signal, Edif1 =  $T_{WL} - T_{WS1}$  (data group C minus group D) data and Edif2 =  $T_{WL} - T_{WS2}$  (A group minus B group) data. Next, Edif1 and Edif2 are used to compute two apparent hydrocarbon volumes by using matched filters to fit exponential terms to each echo difference train. The  $T_1$  for the hydrocarbon phase  $T_{1p1}$  is given by

$$e^{-\frac{T_{WS1}}{T_{1,p1}}} - e^{-\frac{T_{WL}}{T_{1,p1}}} = \frac{A(T_{WS1}, T_{WL}, T_{1,p1})}{e^{-\frac{T_{WS2}}{T_{1,p1}}} - e^{-\frac{T_{WL}}{T_{1,p1}}}} = \frac{A(T_{WS1}, T_{WL}, T_{1,p1})}{A(T_{WS2}, T_{WL}, T_{1,p1})},$$

30



where  $A(T_{ws1}, T_{wl}, T_{l,p1})$  represents the apparent hydrocarbon amplitude from Edif1, and  $A(T_{ws2}, T_{wl}, T_{l,p1})$  is the apparent hydrocarbon amplitude from Edif2, see Eqn. (3) above. For known values of  $T_{wl}$ ,  $T_{ws1}$ ,  $T_{ws2}$  and the apparent hydrocarbon amplitudes from Edif1 and Edif2, the parameter  $T_l$  of the hydrocarbon phase can be determined readily.

5

Case 1: A three-phase mixture of water, light oil (or oil filtrate), and gas.

Matched-filter exponential fitting is performed on the Edif1 and Edif2 echo differences as above to obtain apparent volumes for each of the hydrocarbon phases.  $T_l$ 's for the hydrocarbon phases are given by applying Eqn. (2) separately for oil (phase p1) and gas (phase p2). As before,  $T_l$  values for the hydrocarbons can be computed directly from the known quantities.

10

Based on the above discussion, it is apparent that a key element of the method for determining hydrocarbon  $T_l$  values is the selection of the wait times. Generally, all  $T_w$  values should be long enough to polarize the water signal fully, so that echo difference signals (i.e., Edif1, Edif2, ...) contain only hydrocarbon signals that have discrete  $T_l$  and  $T_2$  values for each phase. In addition, in accordance with the present invention the left side of Eqns. (2) and (3) must be from 1.4 to 5 for  $T_l$  to be accurately determined. Moreover, the delay times must be chosen to keep the overall activation set cycle time as short as possible to maximize logging speed.

15

20

In a typical Gulf of Mexico gas well, water  $T_2$  signals range from a few hundred microseconds to a few hundred milliseconds, and gas  $T_l$ 's are on the order of a few seconds. See, e.g., Akkurt, R., *et al.*: "NMR Logging of Natural Gas Reservoirs," Paper N presented at the 36<sup>th</sup> Annual SPWLA Logging Symposium, Paris, June 26–29, 1995. Fig. 3 shows hypothetical saturation recovery curves for water (assuming  $T_l = 0.25$  s) and hydrocarbon (assuming  $T_l = 3$  s). The uppermost curve is for water with an assumed  $T_l = 0.25$  s. From this, it can be seen that a  $T_w$  of 1 second will achieve more than 95% polarization

25

30

of the water signal. The bottom curve depicts a hydrocarbon phase ( $T_1 = 3$  s). The middle curve represents an equal mixture of the water and hydrocarbon phases. For two-phase mixtures of these fluids, accurate values for hydrocarbon  $T_1$  and volume can be obtained with the triple-wait-time method when wait times of 1, 3, and 8 seconds (indicated by the vertical lines) are used.

5 Shown in Fig. 4 are crossplots of  $T_{ws1}$  and  $T_{ws2}$  with contour lines of

$$F = \left[ e^{-(T_{ws1}/T_1)} - e^{-(T_{wl}/T_1)} \right] / \left[ e^{-(T_{ws2}/T_1)} - e^{-(T_{wl}/T_1)} \right] \quad (5)$$

10 for  $T_1$  values from 3 to 6 seconds. The  $T_{ws2}$ - $T_{ws1}$  crossplots illustrate the selection of triple-wait-time combinations according to the method of the present invention dependent on expected hydrocarbon  $T_1$  values (rows of panels) and long wait times, (columns of panels). Contour lines according to Eqn. (5) start at  $F = 1$  and increase by increments of 0.1 toward the upper left corner in each panel. For good hydrocarbon  $T_1$  determinations,  $F$  should be 1.4 or larger. With  
15 reference to Fig. 4, if a 1-second  $T_w$  ( $T_{ws1}$ ) is needed to fully polarize the water signal and the possible hydrocarbon  $T_1$  could be as large as 6 seconds, then for an 8-second  $T_{wl}$  the charts suggest that  $T_{ws2}$  should be 3 seconds.

In accordance with the present invention, these crossplots can be used in  
20 selecting the best wait-time combination for a given set of logging conditions. For example, based on the above criteria and the information in Figs. 3 and 4, the three  $T_w$  values for a typical Gulf of Mexico well can be selected as 1, 3, and 8 seconds. It should be apparent that for different conditions different  $T_w$  can be selected using the crossplots shown in Fig. 4, or the mathematical relationship  
25 expressed in Eqn. (5). The derivation of these tools is believed to be a significant contribution of the present invention.

### E. Applications

One of the main applications of the system and method of this invention stems from the need to determine accurately the  $T_1$  parameter corresponding to slow  $T_2$  decay components in echo difference signals usually associated with light hydrocarbons, such as light oil, oil filtrate, and gas or free brine in large pores.

- 5 Three experiments were performed with mixtures of  $C_{12}H_{26}$  and doped water, a sandstone core filled with water and  $C_{12}H_{26}$ , and a freshwater-filled tank to demonstrate the effectiveness of the proposed method. A MARAN-1 laboratory spectrometer operating at a 1-MHz resonant frequency was used to obtain measurements on the bulk  $C_{12}H_{26}$ /doped water and sandstone core samples. A  
10 MRIL-Prime logging tool was used to perform experiments in a water-filled tank. The following describes the procedures and results obtained from each experiment.

#### 15 **Mixture of doped water and dodecane.**

- A 3.5-in. (inside diameter) glass sample holder was used to measure bulk fluids in the MARAN spectrometer. To determine the true volumes of the samples in arbitrary units, CPMG pulse sequences were used to make 10 measurements on separate samples of doped water and  $C_{12}H_{26}$ . The mean volume  
20 of the doped water sample was determined to be  $136 \pm 0.7$  arbitrary units. Similarly, the mean volume for the  $C_{12}H_{26}$  sample was found to be  $108 \pm 0.9$  arbitrary units. Inversion recovery measurements, consisting of 51 inversion recovery times, were performed separately on the samples. The data from these experiments were used to find bulk-fluid  $T_1$  values of  $395 \pm 1.8$  and  $995 \pm 4.7$  ms,  
25 respectively, for the doped water and  $C_{12}H_{26}$  samples.

- The samples of doped water and  $C_{12}H_{26}$  were combined and mixed to form a 1.26:1-volume ratio of doped water to  $C_{12}H_{26}$ . A series of tests were performed on the mixture in which different wait-time combinations were used to collect sets of 30 CPMG triple-wait-time experiments consisting of 5,000 1-ms echoes.  
30 Data from these tests were used to derive the  $C_{12}H_{26}$  volumes and  $T_1$ 's that are

shown in Table 1 below for each triple-wait-time combination trial. By comparing the true values with the results in Table 1, the smallest error occurred when a triple-wait-time combination of 1, 2, and 8 seconds was used.

**Table 1—Optimization of  $T_w$ s for determining  $T_1$  and volume of hydrocarbon in a mixture of dodecane and doped water**

	True values	$TW_s=1, 1.5, \& 8\text{ s}$	$TW_s=1, 2, \& 8\text{ s}$	$TW_s=1, 2.5, \& 8\text{ s}$	$TW_s=1, 3, \& 8\text{ s}$
$T_1$ of $C_{12}H_{26}$ (ms)	995 <sup>a</sup>	1162	991	1047	893
Standard dev. of $T_1$ (ms)	4.7	158.1	66.4	74.2	150.9
Volume of $C_{12}H_{26}$ (arb.)	108 <sup>b</sup>	92.9 <sup>c</sup>	106.7 <sup>c</sup>	102 <sup>c</sup>	119.5 <sup>c</sup>
Standard dev. of the volume (arb.)	0.9	3.3	4.0	4.1	7.1

<sup>a</sup>True  $T_1$  was derived from an inversion recovery measurement with 51 inversion recovery times performed on a bulk sample.

<sup>b</sup>Reported sample volume is the average signal amplitude at  $t = 0$  obtained from  $T_2$  inversions performed on 10 CPMG measurements.

<sup>c</sup>The volume of  $C_{12}H_{26}$  in the doped water/ $C_{12}H_{26}$  mixture is the same as the  $C_{12}H_{26}$  sample.

Fig. 5 shows the triple-wait-time echo trains acquired for the 1-, 2-, and 8-second combination. The MAP algorithm was used to perform 21-bin  $T_2$  inversions of the, 8-second wait-time echo trains. Overlay of triple-wait-time echo trains obtained in the laboratory from 30 CPMG experiments performed on a 1.26:1 mixture of doped water and  $C_{12}H_{26}$ . The top set of curves is the 8-second  $T_w$ . The middle set is the 2-second  $T_w$ . The bottom set of curves was acquired with a 1-second  $T_w$ . For details of the MAP algorithm the reader is directed to U.S. Pat. No. 5,517,115; and Prammer, M.G.: "NMR Pore Size Distributions and Permeability at the Well Site," paper SPE 28368 presented at the 1994 SPE Annual Technical Conference and Exhibition, New Orleans, Sept. 25–28, the disclosure of which is hereby incorporated by reference.

An example from one experiment, Fig. 6 shows a uni-modal distribution of  $T_2$  values. This  $T_2$  distribution was selected at random from one of the 8-s  $T_w$  CPMG experiments performed on the doped-water/ $C_{12}H_{26}$  mixture using this invention. A MAP inversion with 21  $T_2$  bins (indicated by the stair-step curve) was performed. The bin amplitudes, shown as the line joining  $T_2$  times at the bin centers, have been normalized to the maximum bin amplitude. The dotted curve indicates the normalized cumulative amplitude as a function of  $T_2$  time. The two liquid phases are not resolved in the  $T_2$  spectrum at the signal-to-noise conditions for the single experiment shown. A similar situation occurs in many logging applications, which can make fluid typing difficult with only one kind of NMR acquisition.

To obtain only  $C_{12}H_{26}$  signals, the triple-wait-time echo trains were used to generate two sets of echo train differences for each experiment, shown in Fig. 7. Fig. 7 shows overlays of difference echo trains for the 30 CPMG triple-wait-time sequences performed on a doped-water/ $C_{12}H_{26}$  mixture. The top panel shows the Edif2 (8-second minus 2-second) differences and the bottom panel shows the Edif1 (8-second - 1-second). In addition, each panel includes the corresponding matched-filter fitted curves that provided the apparent  $C_{12}H_{26}$  volume for each experiment.

Assuming the doped water signals are eliminated in the Edif1 (8-second minus 1-second echo difference) echo train, Edif1 was used to determine the most probable hydrocarbon  $T_2$  value -  $T_{2mp}$ . The value was found by performing  $T_2$  inversions on each Edif1 echo train and computing the average of the largest  $T_2$  modes observed in the 30 distributions.

Apparent  $C_{12}H_{26}$  signal amplitudes,  $A_0$ , in the echo difference trains were obtained for each experiment by fitting the Eqn. (1), reproduced here for convenience

$$A(t) = A_0 e^{-\frac{t}{T_{2mp}}},$$

where  $A(t)$  represents the average echo difference amplitude at echo time  $t$  to both Edif1 and Edif2.

The apparent  $T_1$ 's from the triple-wait-time experiments were found by solving Eq. 1 when  $A(T_{WS1}, T_{WL}, T_{1,pl})$  and  $A(T_{WS2}, T_{WL}, T_{1,pl})$  were replaced with the Edif1 and Edif2  $C_{12}H_{26}$  signal amplitudes, respectively, for each experiment. The most probable  $T_1$  (average of the 30 experiments),  $T_{1mp}$ , was then used to compute corrected hydrocarbon volumes ( $C_{12}H_{26}$ )  $\phi_h$  by applying Eqn. (4)

$$\phi_h = \frac{A_{o, Edif1}}{HI_h \left( e^{-\frac{T_{WS1}}{T_{1mp}}} - e^{-\frac{T_{WL}}{T_{1mp}}} \right)},$$

where  $HI_h$  is the hydrogen index of the hydrocarbon, which is equal to 1 for  $C_{12}H_{26}$ . The average  $T_1$  and its standard deviation along with the average corrected volume and its standard deviation are given in Table 1 above. For the 1, 2, and 8-second wait-time combination, the absolute error for  $T_1$  is 0.4%, and the absolute error for the volume of  $C_{12}H_{26}$  is 1.2%.

#### 15 Sandstone core filled with water and dodecane.

A three-step process was used to prepare 3.5- (diameter) by 4.5-in. sandstone core having 22.06% porosity for laboratory NMR experiments with water and  $C_{12}H_{26}$  pore fluids. The core was cleaned and saturated with a 4% potassium chloride (KCl) brine solution under 1 atmosphere of pressure. Then the sample was desaturated to a capillary pressure of 50 psi, and the brine volume in the core was decreased from 151.9 to 32.4 cm<sup>3</sup>. Under atmospheric conditions, 119.5 cm<sup>3</sup> of  $C_{12}H_{26}$  were added to the sample, and the core was placed in a closed glass sample holder before making NMR measurements.

25 As before, several triple-wait-time combinations were investigated to determine the best set of wait times for the saturation state. Sets of 28 triple-wait-time CPMG pulse sequences were collected, which consisted of 9,000 0.4-ms echoes, for each wait-time combination. Data from these tests were used to derive the  $C_{12}H_{26}$  volumes and  $T_1$ 's that are shown in Table 2 for each wait-time combination tried. The true  $C_{12}H_{26}$   $T_1$  value for these experiments was taken to

be the same as the value determined in the bulk fluid experiments, and true  $C_{12}H_{26}$  volume was normalized to core porosity. By comparing the true values with the results in Table 2, the smallest error occurred when a triple-wait-time combination of 0.4, 1, and 6 seconds was used.

5

**Table 2—Optimization of  $T_w$ s for determining  $T_1$  and volume of hydrocarbon in a sandstone core filled with water and dodecane**

	True values	$TW_s=0.4, 0.8, \& 6\text{ s}$	$TW_s=0.4, 1 \& 6\text{ s}$	$TW_s=0.4, 1.2, \& 6\text{ s}$	$TW_s=0.4, 1.4, \& 6\text{ s}$
$T_1$ of $C_{12}H_{26}$ (ms)	995 <sup>a</sup>	1149	1050	1157	1162
Standard dev. of $T_1$ (ms)	4.7	12.5	12.0	11.6	10.5
Volume of $C_{12}H_{26}$ (arb.)	17.35 <sup>d</sup>	17.09	17.10	16.97	17.02
Standard dev. of the volume (arb.)	0.140	0.060	0.060	0.061	0.073

15

<sup>a</sup>True  $T_1$  was derived from an inversion recovery measurement with 51 inversion recovery times performed on a bulk sample.

<sup>d</sup>Actual  $C_{12}H_{26}$  volume =  $C_{12}H_{26}$  saturation x core porosity.

20

The triple-wait-time echo trains acquired with the 0.4-, 1-, and 6-second combination are displayed in Fig. 8. The figure shows overlay of triple-wait-time echo trains obtained in the laboratory from 28 CPMG experiments performed on a 22-p.u. sandstone core filled with a 4% KCl brine and  $C_{12}H_{26}$ . The top set of curves is the 6-second  $T_w$ . The middle set is the 1-second  $T_w$ . The bottom set of curves was acquired with a 0.4-second  $T_w$ .

25

Fig. 9 shows the results of a 21-bin inversion performed on one of the 6-second  $T_w$  echo trains. The figure illustrates a  $T_2$  distribution, selected at random, from one of the 6-s  $T_w$  measurements performed on the brine- and  $C_{12}H_{26}$ -filled sandstone core. The sharp, high-amplitude peak in the 1,000-ms bin

30

comes from the  $C_{12}H_{26}$ . The two lower amplitude peaks to the left are from the residual brine. The cumulative amplitude ratio (dotted curve) indicates that the volume ratio of  $C_{12}H_{26}$  to water is approximately 4:1, close to the materials balance ratio of 3.7:1.

Edif1 and Edif2 echo differences (shown in Fig.10) were generated from the triple-wait-time echo trains to cancel the residual water signal. The most probable hydrocarbon  $T_2$  was extracted by inverting the Edif1 (6-second minus 0.4-second echo difference) echo trains. More specifically, Fig. 10 shows overlays of difference echo trains for the 28 CPMG triple-wait-time sequences performed on the brine- and  $C_{12}H_{26}$ -filled sandstone core sample. The top panel shows the Edif2 (6-second minus 1-second) differences. The bottom panel shows the Edif1 (6-second minus 0.4-second). Matched-filter fitted curves are also shown for each experiment that provided the apparent  $C_{12}H_{26}$  volume.

Edif1 and Edif2 were each fit to the exponential relationship in Eq. (1) to obtain the apparent  $C_{12}H_{26}$  signal amplitudes that were used in Eq. (3) to compute an apparent  $T_1$  for each CPMG triple-wait-time sequence. Eq. (4) was then used to compute corrected  $C_{12}H_{26}$  volumes for comparison with the true value. The absolute error for  $T_1$  is 5.5%, and the absolute error for the volume of  $C_{12}H_{26}$  is 1.4%. The Edif1 signal-to-noise ratio is defined for the examples in this paper as the first echo difference amplitude divided by the standard deviation of the mean of the last 100 echo difference amplitudes. Edif1 signal-to-noise ratio was approximately 5:1 in this series of experiments, compared with the 7:1 ratio obtained during the bulk fluid mixture experiments discussed previously. The larger errors obtained in this case are attributed to the poorer signal-to-noise quality of the measurements.

#### Freshwater tank.

The triple-wait-time method was also tested by the use of an MRIL-Prime tool in a freshwater-filled tank in which the water has a volume of 100 porosity units (p.u.) and a  $T_1$  of approximately 2.5 seconds.



Again, several wait-time combinations were tried. The activation set shown in Fig. 1 was used to acquire 48 sets of CPMG pulse sequences in the water tank for each wait time combination. In all but frequency 4, the collected echo trains consisted of 400 1.2-ms echoes. Table 3 lists the  $T_1$  and volume results from each test, which show that the optimum combination of wait times for this setup is 1, 3, and 10 seconds.

**Table 3—Optimization of  $T_w$ s for determining  $T_1$  and volume of free fresh water in a water tank**

	True values	$TW_s=1, 3, \& 10$ s	$TW_s=2, 3 \& 10$ s	$TW_s=1, 3.5, \& 12$ s	$TW_s=1.5, 3.5, \& 6$ s
$T_1$ of fresh water (ms)	$\sim 2500^*$	2180	2010	2059	2018
Standard dev. of $T_1$ (ms)		176.2	394.2	170.0	216.2
Volume of $C_{12}H_{26}$ (arb.)	100	100.4	99.6	102	102
Standard dev. of the volume (arb.)		2.43	4.35	2.81	3.13

\*The true  $T_1$  and the volume of the water were obtained in a water tank used to calibrate MRIL-Prime tools.

Though an accurate water volume was obtained from the series of experiments, the water  $T_1$  value obtained with the triple-wait-time method had a relatively large absolute error of 15%. It is believed that the acquisition time of 0.48 seconds (400 echoes x 1.2 ms/echo), which is short compared with the  $T_2$  of bulk water and the 4:1 Edifl signal-to-noise ratio, contributed substantially to this error.

The activation set outlined in Fig. 1, however, has an important advantage over dual-frequency, dual- $T_w$  activations. (See Akkurt, R., *et al.*: "NMR Logging of Natural Gas Reservoirs," Paper N presented at the 36<sup>th</sup> Annual SPWLA Logging Symposium, Paris, June 26–29, 1995). Because four frequencies are

available to collect Edifl echo-difference data, the signal-to-noise quality is 1.4 times better compared with the same data acquired with a dual-frequency activation.

Specifically, Fig. 11 shows how the multifrequency triple-wait-time acquisition method, developed for the MRIL-Prime tool, improves the signal-to-noise ratio of Edifl echo differences compared with those obtained with a dual- $T_w$  dual frequency method. The examples shown were obtained in a freshwater-filled calibration tank. The MRIL-Prime Edifl difference echo trains are displayed in the top panel. The dual- $T_w$  dual frequency Edifl appears in the bottom panel. The multifrequency triple-wait-time method gives an echo difference signal-to-noise ratio that is 1.4 times better. The increase in Edifl signal-to-noise ratio, shown in Fig. 11, is important because it influences the accuracy of  $T_2$ 's,  $T_1$ 's, and volumes of hydrocarbons (or free brine) derived from multi-wait-time measurements.

Based on the above, the inventors have found that the proposed data acquisition and processing method result in substantial improvements over prior art methods. Thus, for NMR signal differences having signal-to-noise ratios larger than 4:1, the absolute errors in determining fluid volume were less than 1.5%. In general, the new acquisition method brings a 1.4-time improvement to echo difference signal-to-noise ratios compared with previous implementations of dual- $T_w$  logging with dual-frequency tools. The triple-wait-time technique has been applied successfully to two-phase or three-phase mixtures of water and hydrocarbons - light oil (or oil filtrate) and gas.

### Mathematical Foundations

The following provides the mathematical foundation for the method outlined above. The time-dependent NMR  $T_2$  signal for a three-phase mixture of oil, gas, and water in a water-wet formation can be expressed as a weighted sum of exponential terms

$$\begin{aligned}
 A(t, T_w) = & HI_g \left( 1 - e^{-\frac{T_w}{T_{1g}}} \right) \sum_i P_g(T_2(i)) e^{-\frac{t}{T_{2(i)}}} \\
 & + HI_o \left( 1 - e^{-\frac{T_w}{T_{1o}}} \right) \sum_i P_o(T_2(i)) e^{-\frac{t}{T_{2(i)}}} \\
 & + \sum_i P_w(T_2(i)) \left( 1 - e^{-\frac{T_w}{T_{1w}(i)}} \right) e^{-\frac{t}{T_{2(i)}}}
 \end{aligned} \tag{A-1}$$

where  $P_g(T_2)$ ,  $P_o(T_2)$ ,  $P_w(T_2)$  are the  $T_2$  incremental porosity spectra of gas, oil and water, respectively. For water,  $T_1$  and  $T_2$  are assumed to be linked through a constant ratio. See, e.g., Kleinberg, R.L., *et al.*: "Nuclear Magnetic Resonance of Rocks:  $T_1$  vs  $T_2$ ," paper SPE 26470 presented at the 1993 SPE Annual Technical Conference and Exhibition, Houston, Oct. 3-6. Therefore, the index of  $T_{1w}$  is correlated with  $T_2$ . If the hydrocarbon signals are limited to singular  $T_2$  times, then Equation A-1 simplifies to

$$\begin{aligned}
 A(t, T_w) = & HI_g \left( 1 - e^{-\frac{T_w}{T_{1g}}} \right) \phi_g e^{-\frac{t}{T_{2g}}} \\
 & + HI_o \left( 1 - e^{-\frac{T_w}{T_{1o}}} \right) \phi_o e^{-\frac{t}{T_{2o}}} \\
 & + \sum_i P_w(T_2(i)) \left( 1 - e^{-\frac{T_w}{T_{1w}(i)}} \right) e^{-\frac{t}{T_{2(i)}}}
 \end{aligned} \tag{A-2}$$

For triple-wait-time method, three similar equations can be used to represent time-dependent signal amplitudes in which the actual wait times are substituted for  $T_w$

$$\begin{aligned}
 A(t, T_{WL}) = & HI_g \left( 1 - e^{-\frac{T_{WL}}{T_{1g}}} \right) \phi_g e^{-\frac{t}{T_{2g}}} \\
 & + HI_o \left( 1 - e^{-\frac{T_{WL}}{T_{1o}}} \right) \phi_o e^{-\frac{t}{T_{2o}}} \\
 & + \sum_i P_w(T_2(i)) \left( 1 - e^{-\frac{T_{WL}}{T_{1w}(i)}} \right) e^{-\frac{t}{T_{2(i)}}}
 \end{aligned} \tag{A-3}$$

$$\begin{aligned}
 A(t, T_{WS1}) = & HI_g \left( 1 - e^{-\frac{T_{WS1}}{T_{1g}}} \right) \phi_g e^{-\frac{t}{T_{2g}}} \\
 & + HI_o \left( 1 - e^{-\frac{T_{WS1}}{T_{1o}}} \right) \phi_o e^{-\frac{t}{T_{2o}}} \\
 & + \sum_i P_w(T_2(i)) \left( 1 - e^{-\frac{T_{WS1}}{T_{1w}(i)}} \right) e^{-\frac{t}{T_{2(i)}}}
 \end{aligned} \tag{A-4}$$

$$\begin{aligned}
 A(t, T_{WS2}) = & HI_g \left( 1 - e^{-\frac{T_{WS2}}{T_{1g}}} \right) \phi_g e^{-\frac{t}{T_{2g}}} \\
 & + HI_o \left( 1 - e^{-\frac{T_{WS2}}{T_{1o}}} \right) \phi_o e^{-\frac{t}{T_{2o}}} \\
 & + \sum_i P_w(T_2(i)) \left( 1 - e^{-\frac{T_{WS2}}{T_{1w}(i)}} \right) e^{-\frac{t}{T_{2(i)}}}
 \end{aligned} \tag{A-5}$$

Models of the time-dependent signals in the Edif1 and Edif2 echo difference trains are obtained when Eqs. A-4 and A-5 are subtracted from Eq. A-3,

$$\begin{aligned}
 \text{Edif1}(t) = & HI_g \phi_g \left( e^{-\frac{T_{WS1}}{T_1}} - e^{-\frac{T_{WL}}{T_1}} \right) e^{-\frac{t}{T_1}} \\
 & + HI_o \phi_o \left( e^{-\frac{T_{WS1}}{T_{1o}}} - e^{-\frac{T_{WL}}{T_{1o}}} \right) e^{-\frac{t}{T_{1o}}} \\
 & + \sum_i P_w(T_2(i)) \left( e^{-\frac{T_{WS1}}{T_{1w}(i)}} - e^{-\frac{T_{WL}}{T_{1w}(i)}} \right) e^{-\frac{t}{T_{2(i)}}}
 \end{aligned} \tag{A-6}$$

$$\begin{aligned}
 \text{Edif2}(t) = & HI_g \phi_g \left( e^{-\frac{T_{WS2}}{T_1}} - e^{-\frac{T_{WL}}{T_1}} \right) e^{-\frac{t}{T_1}} \\
 & + HI_o \phi_o \left( e^{-\frac{T_{WS2}}{T_{1o}}} - e^{-\frac{T_{WL}}{T_{1o}}} \right) e^{-\frac{t}{T_{1o}}} \\
 & + \sum_i P_w(T_2(i)) \left( e^{-\frac{T_{WS2}}{T_{1w}(i)}} - e^{-\frac{T_{WL}}{T_{1w}(i)}} \right) e^{-\frac{t}{T_{2(i)}}}
 \end{aligned} \tag{A-7}$$

When  $T_{WS1}$  is much larger than the maximum water  $T_1$  value, then contributions to Edif1 and Edif2 from under-polarized water become negligible and the last term in Eqs. A-6 and A-7 disappears. The product of hydrogen index, hydrocarbon porosity, and the differential polarization factor represents the amplitude of the hydrocarbon signal. Thus, Eqs. A-6 and A-7 simplify to bi-exponential equations

$$\begin{aligned}
 Edif1(t) = & A_g(T_{WS1}, T_{WL}, T_{lg}) e^{-\frac{t}{T_{2g}}} \\
 & + A_o(T_{WS1}, T_{WL}, T_{lg}) e^{-\frac{t}{T_{2o}}}
 \end{aligned}
 \tag{A-8}$$

$$\begin{aligned}
 Edif2(t) = & A_g(T_{WS2}, T_{WL}, T_{lg}) e^{-\frac{t}{T_{2g}}} \\
 & + A_o(T_{WS2}, T_{WL}, T_{lg}) e^{-\frac{t}{T_{2o}}}
 \end{aligned}
 \tag{A-9}$$

The hydrocarbon signal amplitudes in the Edif1 and Edif2 difference echo trains models can be obtained by applying matched-filter exponential fitting. Once the amplitudes have been determined for the two echo difference trains, the hydrocarbon  $T_i$ 's can be calculated by taking their ratio. The hydrocarbon index and hydrocarbon porosity are canceled when the amplitude ratio is computed so that, for either hydrocarbon phase:

$$\frac{A_h(T_{WS1}, T_{WL}, T_{lh})}{A_h(T_{WS2}, T_{WL}, T_{lh})} = \frac{e^{-\frac{T_{WS1}}{T_{lh}}} - e^{-\frac{T_{WL}}{T_{lh}}}}{e^{-\frac{T_{WS2}}{T_{lh}}} - e^{-\frac{T_{WL}}{T_{lh}}}}
 \tag{A-10}$$

For the reader's convenience, a list of all notations used in the description above is given next.

### Nomenclature

5	A	-	amplitude, p.u.
	D	-	self-diffusion coefficient, cm <sup>2</sup> /s
	<i>Edif1</i>	-	echo train difference from T <sub>WL</sub> and T <sub>WS1</sub> data, p.u.
	<i>Edif2</i>	-	echo train difference from T <sub>WL</sub> and T <sub>WS2</sub> data, p.u.
	F	-	contour constant
	HI	-	hydrogen index
10	P	-	incremental porosity
	t	-	time, s
	T <sub>1</sub>	-	longitudinal NMR relaxation time, s
	T <sub>2</sub>	-	transverse NMR relaxation time, s
	T <sub>e</sub>	-	echo spacing, ms
	T <sub>w</sub>	-	wait-time, s
15	T <sub>WL</sub>	-	long wait time in the triple-wait-time method, s
	T <sub>WS1</sub>	-	shortest wait time in the triple-wait-time method, s
	T <sub>WS2</sub>	-	second shortest wait time in the triple-wait-time method, s
	φ	-	porosity
20	Subscripts		
	bvi	-	capillary-bound water
	cbw	-	clay-bound water
	g	-	gas
	h	-	hydrocarbon
25	mp	-	most probable
	o	-	oil
	p1	-	fluid phase one
	p2	-	fluid phase two
	pw	-	produced water
30	t	-	total

ta - total apparent  
w - water

While the invention has been described with reference to a preferred embodiment, it will be appreciated by those of ordinary skill in the art that  
5 modifications can be made to the structure and form of the invention without departing from its spirit and scope which is defined in the following claims.

10

15

20

25

30



What is claimed is:

1. A nuclear magnetic resonance (NMR) data acquisition method, comprising:

providing a first set of CPMG pulses associated with a first relatively short recovery time  $T_{WS1}$ ;

5

providing a second set of CPMG pulses associated with a second relatively short recovery time  $T_{WS2}$ , where  $T_{WS2}$  is longer than  $T_{WS1}$ ;

providing a third set of CPMG pulses associated with a relatively long recovery time  $T_{WL1}$ ;

10

receiving NMR echo signals from a population of particles in response to the first, second and third sets of CPMG pulses; and

processing the received NMR echo signals to provide a data representation associated with the longitudinal relaxation time constant  $T_1$  of the population of particles.

15

2. The method of claim 1 wherein the steps of providing the first, second and third sets of CPMG pulses are interleaved in time.

3. The method of claim 1 wherein NMR echo signals received from at least two of the first, second and third sets of CPMG pulses are acquired in different sensitive volumes.

20

4. The method of claim 1 wherein the NMR echo signals received from the first set of CPMG pulses are partially recovered.

5. The method of claim 1 wherein the steps of providing the first, second and third sets of CPMG pulses are performed using a multi-frequency NMR logging tool.

25

6. The method of claim 1 wherein the first and the second sets of CPMG pulses have different operating frequencies.

30

7. The method of claim 1 further comprising the step of providing a fourth set of CPMG pulses associated with a second relatively long recovery time  $T_{WL2}$ .

8. The method of claim 7 wherein the third and the fourth sets of CPMG pulses have different operating frequencies.

5 9. The method of claim 7 wherein at least one set of CPMG pulses associated with a relatively short recovery time and at least one set of CPMG pulses associated with a relatively long recovery time have the same operating frequency.

10 10. The method of claim 1 wherein for at least one of the first, second and third sets of CPMG pulses one or more corresponding sets of CPMG pulses with the same recovery time are provided at a different operating frequency.

11. The method of claim 1 wherein the first and second relatively short recovery times  $T_{WS1}$  and  $T_{WS2}$  are selected long enough to substantially polarize a water phase component in the population of particles.

12. The method of claim 1 wherein the recovery times  $T_{WS1}$ ,  $T_{WS2}$  and  $T_{WL1}$  of the first, second and third sets of CPMG pulses are selected such that water-phase contribution is substantially canceled in a difference signal formed by subtracting NMR signals corresponding to a relatively short recovery time from NMR signals corresponding to the relatively long recovery time  $T_{WL1}$ .

13. The method of claim 1 wherein the first, second and third sets of CPMG pulses are applied in three different frequency bands.

25

30

14. A method for conducting NMR logging measurements, comprising:  
providing a data acquisition sequence comprising at least two sets of CPMG pulses having relatively short recovery times  $T_{WS1}$  and  $T_{WS2}$ , respectively, and at least one set of CPMG pulses having relatively long recovery time  $T_{WL1}$ ;  
receiving NMR echo signals from a population of particles in a geologic formation in response to the provided sets of CPMG pulses;  
processing the received NMR echo signals to determine a first and a second apparent volumes for at least one hydrocarbon fluid phase of the geologic formation, said first apparent volume being determined from a data representation associated with signals having short recovery time  $T_{WS1}$ , and the second apparent volume being determined from a data representation associated with signals having short recovery time  $T_{WS2}$ ;  
providing a data representation associated with the longitudinal relaxation time constant  $T_1$  of said at least one hydrocarbon fluid phase based on the determined first and second apparent volumes.
15. The method of claim 14 wherein the step of processing the received NMR echo signals comprises:  
forming a first difference signal  $Edif1$  by subtracting NMR signals having relatively short recovery time  $T_{WS1}$  from NMR echo signals having relatively long recovery time  $T_{WL}$ .
16. The method of claim 15 further comprising the step of computing  $T_2$  distribution of the first difference signal  $Edif1$ .
17. The method of claim 16 further comprising determining a value for the  $T_2$  relaxation time of said at least one hydrocarbon phase.
18. The method of claim 17 wherein the value for the  $T_2$  relaxation time is determined as the most probable value based on the  $T_2$  distribution of the first difference signal  $Edif1$ .
19. The method of claim 17 further comprising the step of:

forming a second difference signal Edif2 by subtracting NMR signals having relatively short recovery time  $T_{WS2}$  from NMR echo signals having relatively long recovery time  $T_{WL}$ .

20. The method of claim 19 wherein the step of determining a first and second apparent volumes for said at least one hydrocarbon phase are based on the determined value for the  $T_2$  relaxation time and the first and second difference signals Edif1 and Edif2.

21. The method of claim 20 wherein the step of determining said first and second apparent volumes is performed using matched filters to fit a model of the signal to each difference signal Edif1 and Edif2.

22. The method of claim 20 wherein the step of determining a first and second apparent volumes for said at least one hydrocarbon phase trains is performed by fitting the equation:

$$A(t) = A_0 e^{-\frac{t}{T_{2mp}}},$$

where  $A(t)$  represents the average echo difference amplitude Edif1 and Edif2 at echo time  $t$  and  $T_{2mp}$  is the most probable amplitude  $T_2$  value for the hydrocarbon phase.

23. The method of claim 20 wherein the step of providing a data representation associated with the longitudinal relaxation time constant  $T_1$  comprises: for each of said at least one hydrocarbon fluid phase solving the following equation for the corresponding  $T_{1,pi}$  parameter:

$$\frac{e^{-\frac{T_{WS1}}{T_{1,pi}}} - e^{-\frac{T_{WL}}{T_{1,pi}}}}{e^{-\frac{T_{WS2}}{T_{1,pi}}} - e^{-\frac{T_{WL}}{T_{1,pi}}}} = \frac{A(T_{WS1}, T_{WL}, T_{1,pi})}{A(T_{WS2}, T_{WL}, T_{1,pi})}$$

where  $A(T_{WS1}, T_{WL}, T_{1,pi})$  represents the apparent hydrocarbon amplitude of the  $i$ th hydrocarbon phase from Edif1, and  $A(T_{WS2}, T_{WL}, T_{1,pi})$  is the apparent hydrocarbon amplitude of the  $i$ th hydrocarbon phase from Edif2.

24. The method of claim 23 further comprising the step of computing corrected hydrocarbon volumes based on the computed value for the  
5 corresponding  $T_1$  parameter of said at least one hydrocarbon fluid phase.

25. The method of claim 24, wherein the corrected volumes are computed using the equation:

$$10 \quad \phi_i = \frac{A_{o,Edif1}}{HI_i \left( e^{-\frac{T_{WS1}}{T_{1mp}}} - e^{-\frac{T_{WL}}{T_{1mp}}} \right)},$$

where  $HI_i$  is the hydrogen index for the  $i$ th hydrocarbon phase.

15 26. The method of claim 14 further comprising the step of computing the total apparent porosity  $\phi_{ta}$  of the geologic formation.

27. The method of claim 26 further comprising the step of determining the total porosity of the formation  $\phi_t$  from the total apparent porosity  $\phi_{ta}$  and apparent volume corrections computed based on the provided data representation  
20 associated with the longitudinal time constant(s)  $T_1$  of the fluid phases.

28. The method of claim 27 further comprising the step of determining the total water volume as the difference between the total porosity and porosity associated with hydrocarbon phases.

25

29. A method of operating a multi-volume NMR logging tool, comprising:

(a) acquiring a first NMR echo train or sets of echo trains in a first sensitive volume of the tool, said first echo train(s) carrying information about  
30 NMR signals with recovery time  $T_{WS1}$ ;

(b) acquiring a second NMR echo train or sets of echo trains in a second sensitive volume of the tool, said second echo train(s) carrying information about NMR signals and having recovery time  $T_{WL}$ ;

(c) acquiring a third NMR echo train or sets of echo trains, said third echo train(s) carrying information about NMR signals with recovery time  $T_{WS2}$ ;

5 (d) computing values for the transverse relaxation time  $T_2$  and apparent volume for at least one hydrocarbon fluid phase based on the acquired NMR echo trains; and

(e) providing a data representation associated with the longitudinal relaxation time constant  $T_1$  of said at least one hydrocarbon fluid phase based on  
10 the determined first and second apparent volumes.

30. A nuclear magnetic resonance (NMR) data processing method for use in borehole logging, comprising:

15 selecting values for a second relatively short recovery time  $T_{WS2}$  using a known functional relationship based on estimates of: (a) a first relatively short recovery time  $T_{WS1}$  needed to polarize water signals in a geologic formation surrounding the borehole; and (b) expected  $T_1$  values for hydrocarbon fluid phases in the geologic formation surrounding the borehole;

20 providing a data acquisition sequence comprising at least two sets of CPMG pulses having said relatively short recovery times  $T_{WS1}$  and  $T_{WS2}$ , respectively, and at least one set of CPMG pulses having relatively long recovery time  $T_{WL}$ ;

25 processing NMR echo signals received in response to the data acquisition sequence to provide an estimate of the true values for the longitudinal relaxation time constant  $T_1$  of hydrocarbon fluid phases in the geologic formation, wherein the accuracy of the estimates of the  $T_1$  constant is controlled in the step of selecting.

30

processing the received NMR echo signals to provide a data representation associated with the longitudinal relaxation time constant  $T_1$  of the population of particles.

31. The method of claim 30, wherein the known functional relationship is of the form:

5

$$F = \left[ e^{-(T_{WS1}/T_1)} - e^{-(T_{WL}/T_1)} \right] / \left[ e^{-(T_{WS2}/T_1)} - e^{-(T_{WL}/T_1)} \right]$$

where F is a constant.

10

32. The method of claim 31 wherein the value of the constant F is selected greater than about 1.4.

33. The method of claim 31 wherein the value of the constant F is selected in the range between about 1.4 and 5.

15

34. The method of claim 31 wherein the functional relationship is expressed as  $T_{WS1} - T_{WS2}$  cross-plots for select values of the expected  $T_1$  constant and the  $T_{WL}$  relaxation time.

20

35. The method of claim 31 wherein the functional relationship is programmed in a computer memory and the step of selecting is performed automatically based on the values of the expected  $T_1$  constant and the  $T_{WL}$  relaxation time.

25

36. A computer software product for implementing the steps of the method of claim 30 on a computer controlling the operation of a NMR logging tool.

30

Frequency

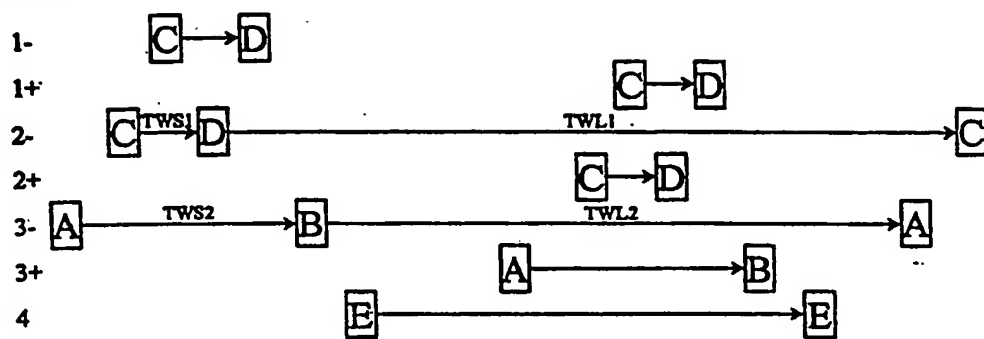


Fig. 1



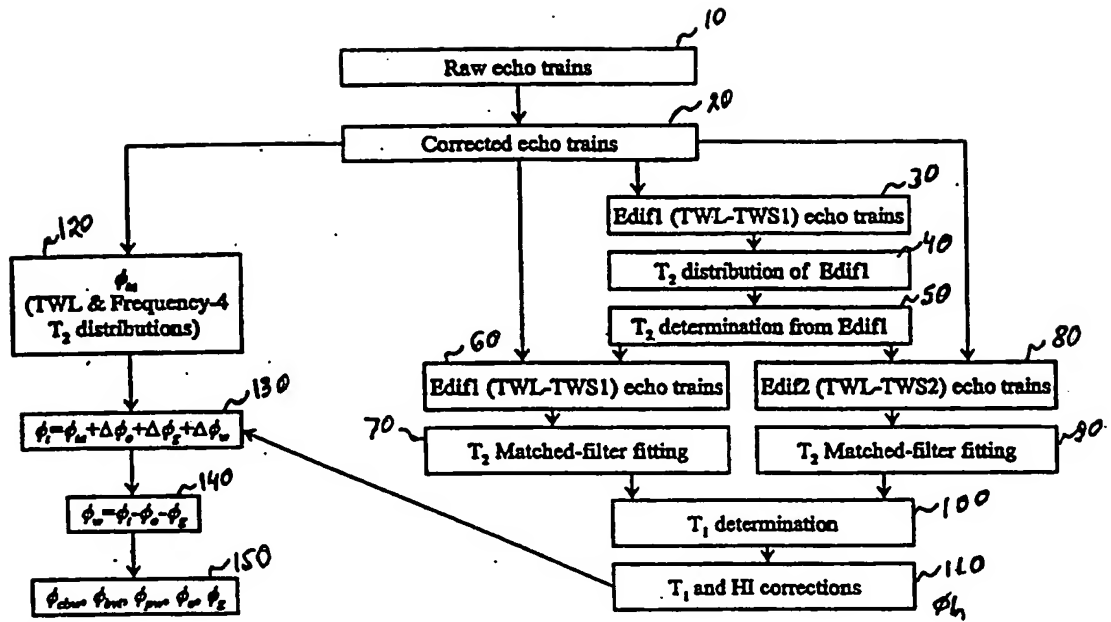


Fig. 2

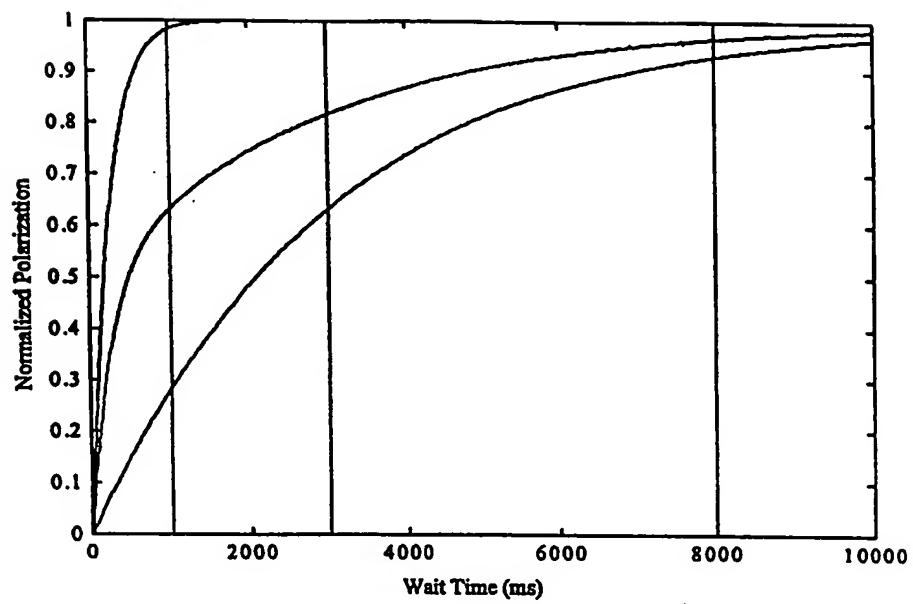


Fig. 3

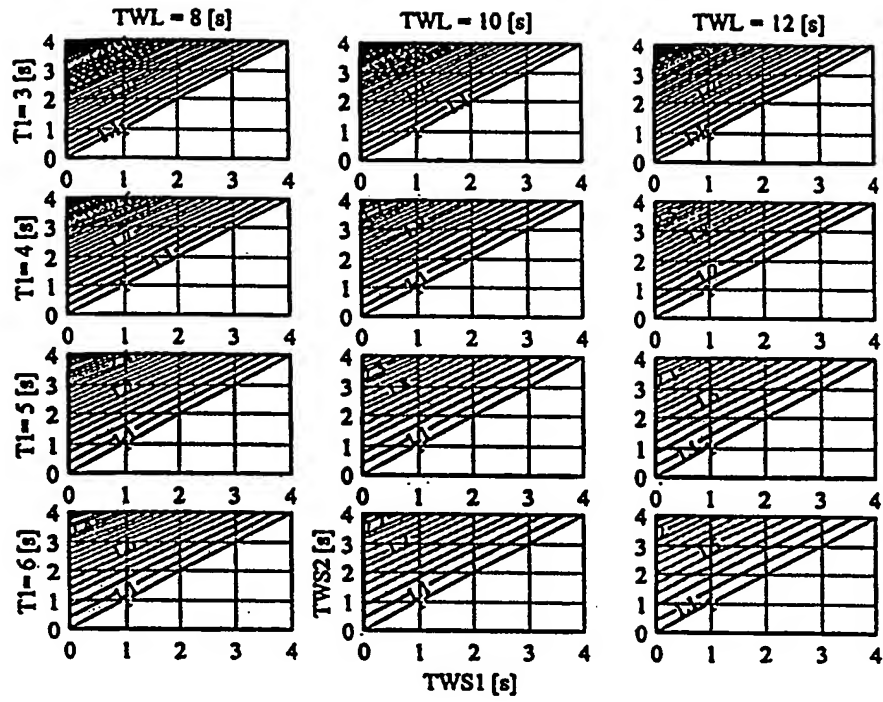


Fig. 4

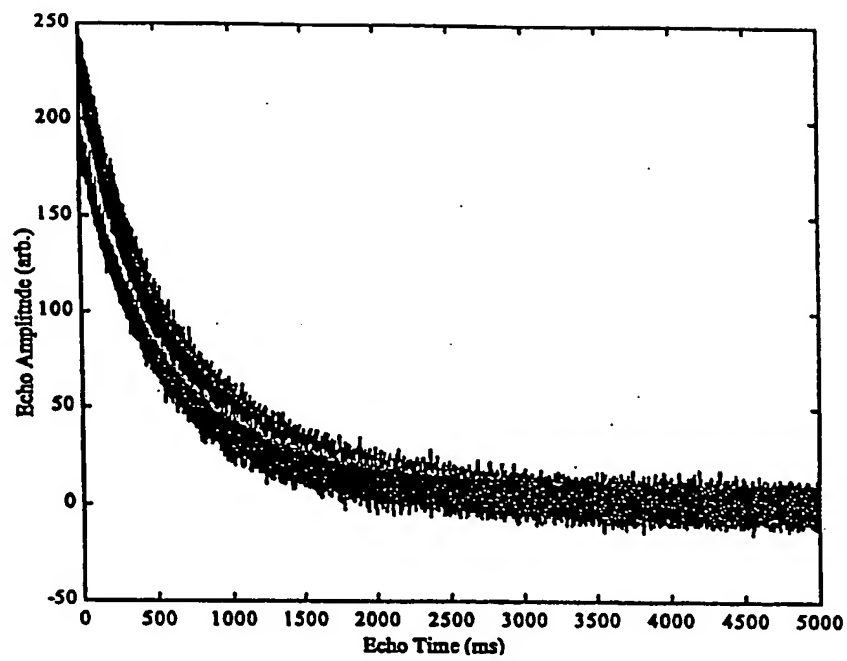


Fig. 5

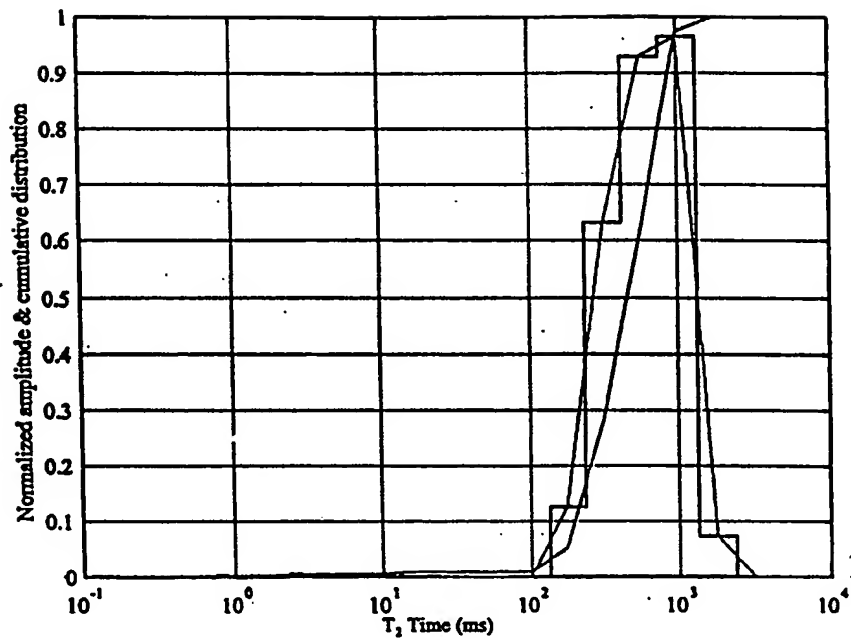


Fig. 6

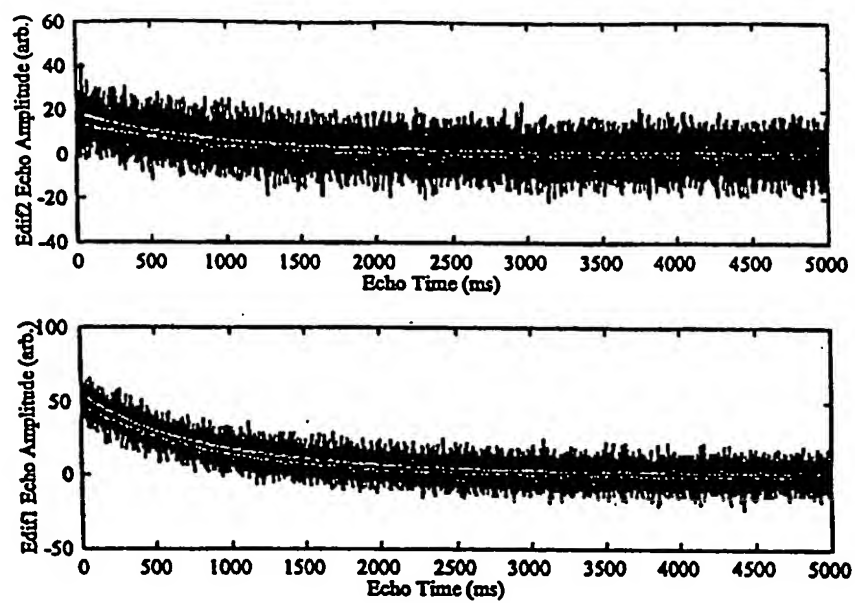


Fig. 7

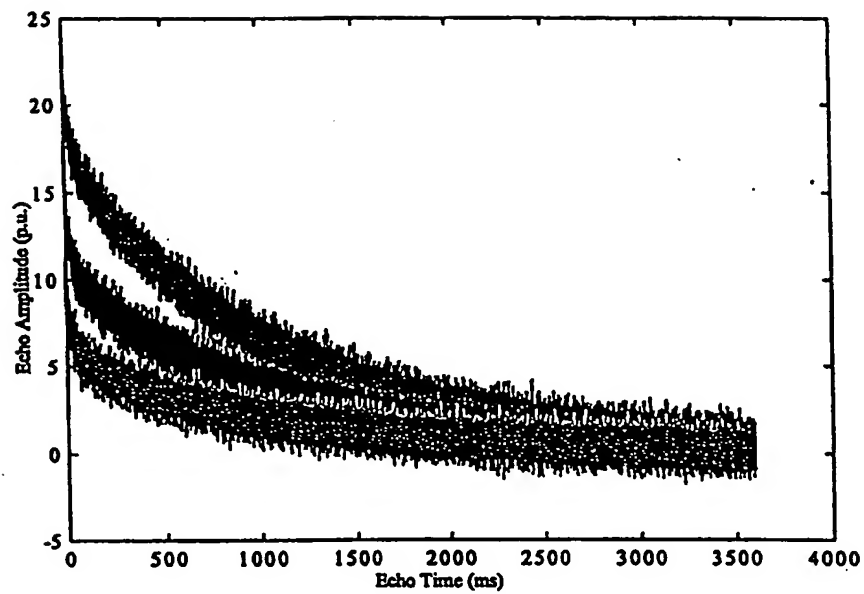


Fig. 8

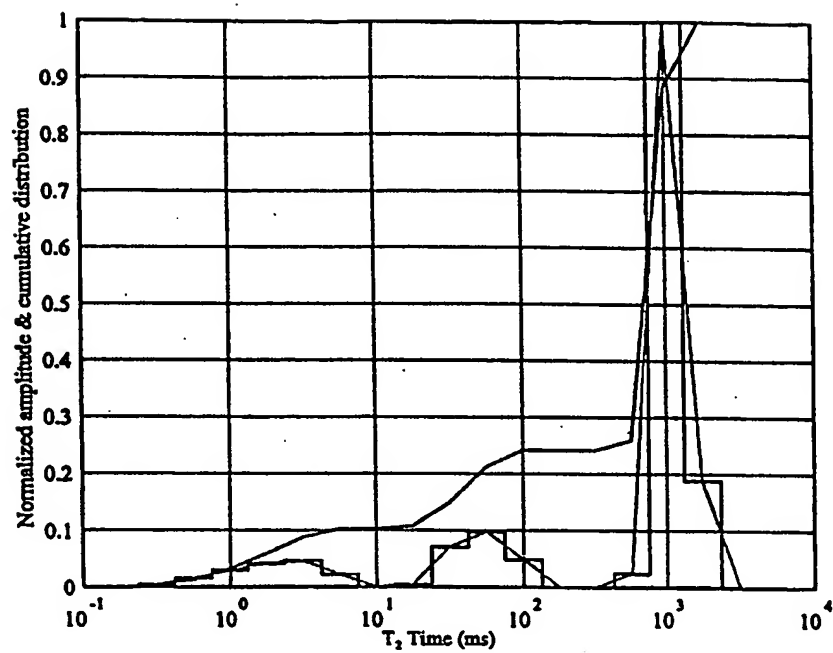


Fig. 9



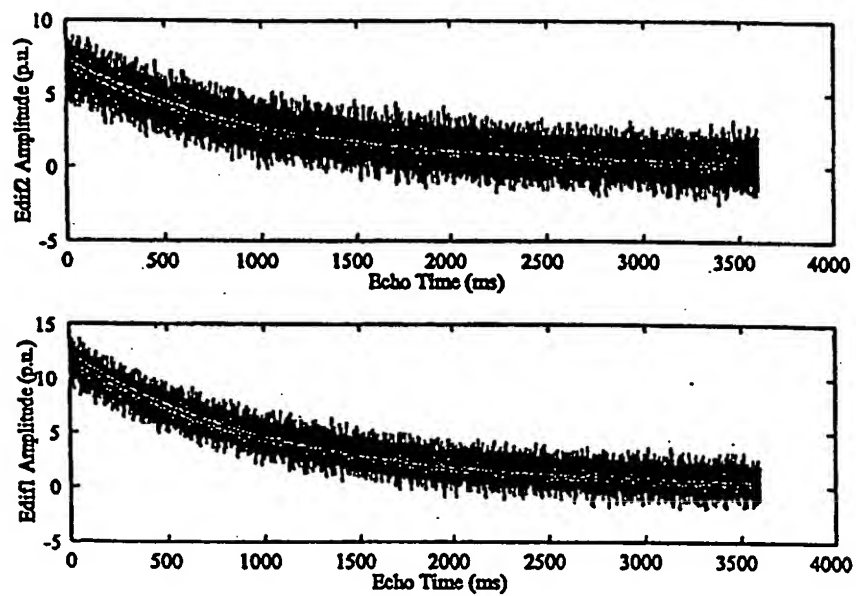


Fig. 10

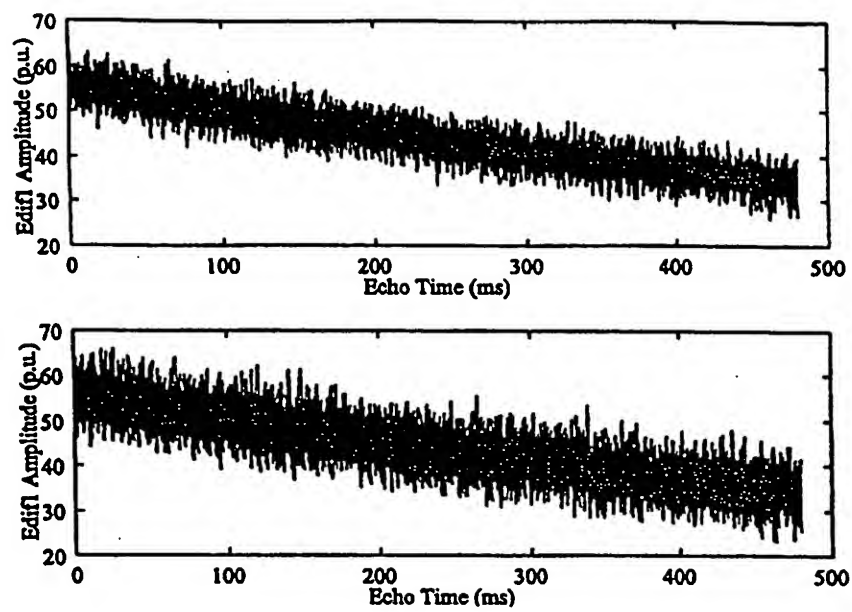


Fig. 11

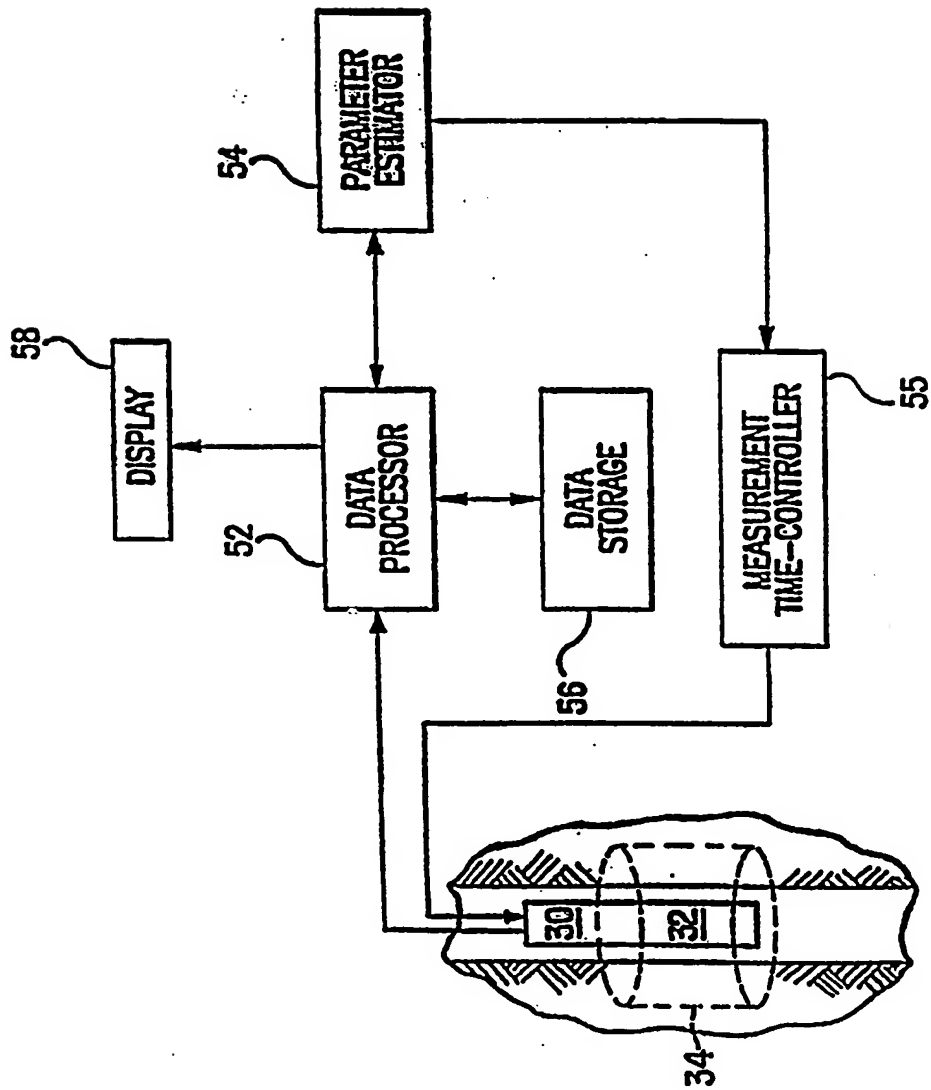


FIG. 12

# INTERNATIONAL SEARCH REPORT

International application No.

PCT/US00/22252

## A. CLASSIFICATION OF SUBJECT MATTER

IPC(7) : G01V 3/00

US CL : 324/303

According to International Patent Classification (IPC) or to both national classification and IPC

## B. FIELDS SEARCHED

Minimum documentation searched (classification system followed by classification symbols)

U.S. : 324/303, 300, 306, 307, 309, 314

Documentation searched other than minimum documentation to the extent that such documents are included in the fields searched

Electronic data base consulted during the international search (name of data base and, where practicable, search terms used)  
EAST

## C. DOCUMENTS CONSIDERED TO BE RELEVANT

Category *	Citation of document, with indication, where appropriate, of the relevant passages	Relevant to claim No.
X	US 5,023,551 A (KLEINBERG et al) 11 June 1991 (11.06.1991), col 18, lines 22-68, col 19, lines 1-4.	1-36
A,P	US 6,049,205 A (TAICHER et al) 11 April 2000 (11.04.2000), see Fig. 2 and Fig.3 and the abstract of the disclosure.	1-36

☐ Further documents are listed in the continuation of Box C.

☐ See patent family annex.

\* Special categories of cited documents:

"A" document defining the general state of the art which is not considered to be of particular relevance

"E" earlier application or patent published on or after the international filing date

"L" document which may throw doubts on priority claim(s) or which is cited to establish the publication date of another citation or other special reason (as specified)

"O" document referring to an oral disclosure, use, exhibition or other means

"P" document published prior to the international filing date but later than the priority date claimed

"T"

later document published after the international filing date or priority date and not in conflict with the application but cited to understand the principle or theory underlying the invention

"X"

document of particular relevance; the claimed invention cannot be considered novel or cannot be considered to involve an inventive step when the document is taken alone

"Y"

document of particular relevance; the claimed invention cannot be considered to involve an inventive step when the document is combined with one or more other such documents, such combination being obvious to a person skilled in the art

"&"

document member of the same patent family

Date of the actual completion of the international search

28 September 2000 (28.09.2000)

Name and mailing address of the ISA/US

Commissioner of Patents and Trademarks  
Box PCT  
Washington, D.C. 20231

Facsimile No. (703)305-3230

Date of mailing of the international search report

21 Dec 2000  
Authorized officer

Louis Arana

Telephone No. (703) 305-4913